GEOLOGIJA *56/1*, 107-128, Ljubljana 2013

doi:10.5474/geologija.2013.009

Mineral chemistry and genesis of Zr, Th, U, Nb, Pb, P, Ce and F enriched peralkaline granites of El-Sibai shear zone, Central Eastern Desert, Egypt

Mohamed A. ALI

Nuclear Materials Authority P. O. Box: 530 El-Maadi, Cairo, Egypt; e-mail: dr_mohamed1966@yahoo.com

Prejeto / Received 3. 8. 2011; Sprejeto / Accepted 20. 5. 2013

Key words: Thorite, zircon, zirconolite, cerite-(Ce), El-Sibai peralkaline granite, electron probe microanalyses, hydrothermal fluids, Central Eastern Desert, Egypt.

Abstract

El-Sibai mineralized shear zone trending NNE-SSW is located at the northern segment of Gabal El-Sibai (500 m in length and 0.5 to 1.5 m in width). Rocks along the shear zone show different types of alterations such as hematization, kaolinitization, fluoritization, and silicification. These alterations are good traps for rare metals of thorite, ferrocolumbite, pyroclore, plumbopyroclore, fluorite, cerite-(Ce), zircon, Th-rich zircon, zirconolite (mixture of zircon & columbite), fluorapatite, titanite, and monazite minerals.

The detailed mineralogical study of the El-Sibai shear zone revealed its enrichment in Th, Zr, Nb, Pb, U, F, P, LREE (Ce), especially concerning the hematization processes. The close correlation of ferruginated (hematitized) samples with high radioactivity is related to the high ability of iron oxides for adsorption of radioactive elements from their solutions. The rare-metal minerals found in altered peralkaline granites (shear zone) are associated with hematitization, albititization, chloritization, fluoritization, and pyritization. Electron probe microanalysis (EPMA) provides an indication of a range of solid solution between thorite and zircon, in which intermediate phases, such as Th-rich zircon were formed. These phases have higher sum of all cations per formula (2.0 to 2.09 atoms per formula unit, for 4 oxygen atoms) than that of ideal thorite and zircon. This is attributed to the presence of substantial amount of interstitial cations such as U, Y, Ca, and Al in these phases. Altered zircon enriched in Th and U (Th-rich zircon) preferentially involves coupled substitution $Ca^{2+} + (Th,U)^{4+} \leftrightarrow 2Zr^{4+} + 2Si^{4+}$, implying that significant amount of U and Th may enter the Zr and Si position in zircon.

Thorite and Th-rich zircon are related to hydrothermal fluid. Also the genesis of the studied zircon is related to metasomatic hydrothermal zircon (MHZ). The abundantly detected zircon, Th-rich zircon, Th-bearing minerals and fluorite of demonstrably hydrothermal origin can be attributed to the role of fluorine-rich fluids. Although Zr and Th are generally considered as highly immobile elements, yet the occurrence of zircon indicates that their significant concentrations can be transported under specified F-rich fluids. The hydrothermal origin could be accepted for the thorite, huttonite monazite, zircon, Th-rich zircon, ferrocolumbite, pyroclore, plumbopyrochlore, zirconolite, fluorite, cerite-(Ce), fluorapatite within the El-Sibai altered peralkaline granites (shear zone).

Introduction

Egyptian granitic rocks of Pan-African age occupy about 40 % of the exposed Precambrian of the Eastern Desert and Sinai. They are subdivided into two distinct major groups, namely the Older and the Younger granites. The Older granites have been referred to in the Egyptian literature as Grey granites (Hume, 1935; El-Ramly & Akaad, 1960), syn- to late-orogenic plutonites (El-Shazly, 1964), synorogenic granites (El-Gaby, 1975) and G1-granites (Hussein et al., 1982). They were emplaced around 930-850 Ma ago, and possibly extend to 711 Ma (El-Manharawy, 1977; Stern & Hedge, 1985; Hassan & Hashad, 1990). On the other hand, the younger granites (about 30 %) were previously mapped as Gattarian granites (Hume, 1935), red and pink granites (El-Ramly & Akaad, 1960), late- to post-orogenic granites (El-Gaby, 1975) and G-II to G-III granites (Hussein et al., 1982). They were emplaced around 622-430 Ma ago (El-Manharawy, 1977; Stern & Hedge, 1985; Hassan & Hashad, 1990; Moghazi et al., 2004; Moussa et al., 2008, Ali & Lentz, 2011).

Shear zones are known to represent important mechanical weaknesses that affect the geology of the continental lithosphere as a kinematic response to deformation (Butler et al., 1995). Stern (1985) and Sultan et al. (1988) suggested through their compilation of Landsat thematic mapper scenes of the Arabian-Nubian Shield (ANS) that the Najd system extends into the Egyptian Eastern Desert and dominates the structural pattern within its central part. Greiling et al. (1993) believed that shear zones in the Pan African basement of the Eastern Desert may be related to compressional as well as extensional stresses; however, both types of deformation led to formation of antiformal structures on a regional scale.

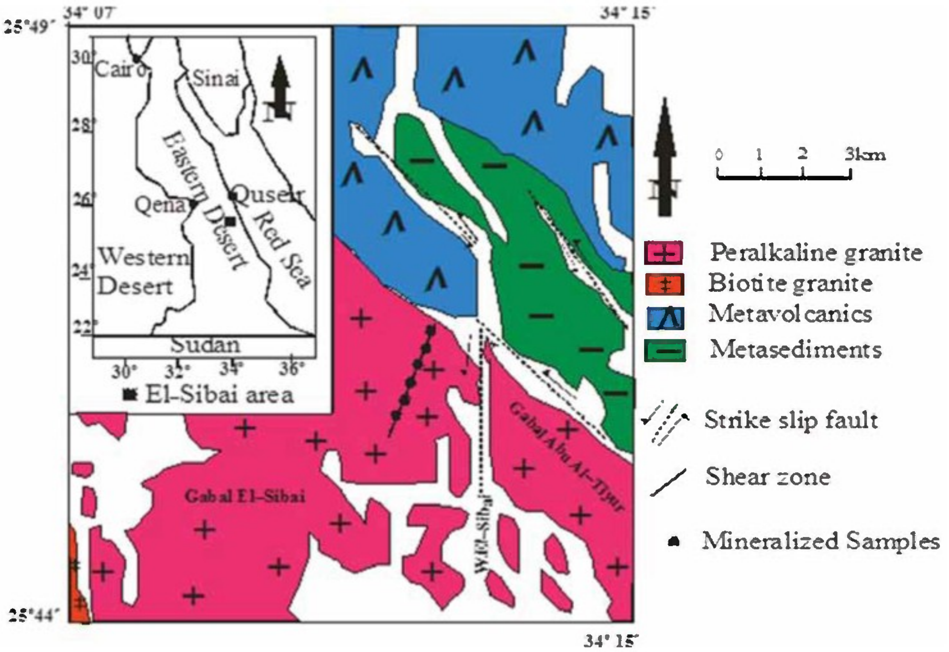

Fig. 1. Geological map of Gabal El-Sibai peralkaline granite (shear zone), Central Eastern Desert, Egypt (modified after Ali, 2001).

Kamal El-Din (1991) described Gabal El-Sibai swell as a doubly plunging anticline trending NW-SE, where the core is occupied by Pre-Pan-African gneisses intercalated in the upper parts by amphibolites. Recently, Ali (2001) delineated a NNE-SSW shear zone at Gabal El-Sibai peralkaline granite (Fig. 1). Abdel-Fattah et al. (2001) studied the anorogenic magmatism; chemical evolution of the Mount El-Sibai A-Type complex (Egypt) and implications for the origin of within-plate felsic magmas. Moussa (2001) studied Gabal El-Sebai alkali feldspar granite and its potentiality to host U-Th mineralization. Earlier geochronological studies indicate that El-Sibai complex is dated at 455 Ma (whole rock K-Ar method) and at 525 Ma (mica K-Ar method): both ages were determined by El-Ramly (1962).

Geochemical studies of the El-Sibai area, including the mineralized shear zone were carried out by Abdel Kader et al. (2001), who concluded that the younger granites are classified into the following types: a) biotite granites and b) alkali-feldspar granites. The biotite granites are classified as monzo-to syenogranites, weakly to mildly alkaline, peraluminous of differentiated I-types, of post orogenic volcanics arc tectonic setting. While the alkali-feldspar granites (El-Sibai granites) are strongly alkaline to peralkaline, A_1-type is rift-related anorogenic (within plate granites or WPG).

Ibrahim et al. (2003) studied the mineralogical and spectrometric characteristics of El-Sibai shear zone and found that the studied shear zone was affected by different types of hydrothermal solutions. Their average eU contents are 38, 29 and 21 ppm, whereas eTh averages 339, 156 and 115 ppm in ferruginated, kaolinized and silicified parts, respectively. Mineralogically, the high level of radioactivity in the shear zone is attributed to the presence of some radioactive minerals, in example plumbobetafite and uranophane as U-bearing minerals, thorite and uranothorite as Th-bearing minerals, zircon, fluorite, galena, magnetite and ilmenite as accessory minerals. In this paper we briefly report on the new mineralogical data obtained with the scanning electron microscope (SEM) and mineral chemistry with EPMA of mineralizations of the El-Sibai altered granites (shear zone).

Analytical methods

Six mineralized samples of the El-Sibai altered peralkaline granites (shear zone) were investigated in details regarding mineralogy and mineral chemistry. Polished thin sections were investigated in reflected and transmitted light in order to determine mineral association and parageneses. Backscattered electron images (BSE) were obtained with the scanning electron microscope (JEOL JSM 6400 SEM), equipped with energy dispersive X-ray spectrometry (EDS) at the Microscopy and Microanalyses Facility, University of New Brunswick (UNB), Fredericton, New Brunswick, Canada. Mineral compositions were determined on the JEOL JXA-733 Superprobe (EPMA); operating conditions were 15 kV, with a beam current of 50 nA and the spectra acquisition time was 30 s. As mineral standards jadeite, kaersutite, quartz, and apatite (for Na, Al, Si, P, and Ca, respectively), $SrTiO_3$ (for Ti), CaF_2 (for F), Fe, Nb, Hf, Ta, Sn, Th, and U metals (for Fe, Nb, Hf, Ta, Sn, Th, and U, respectively), YAG (for Y), cubic zirconia (for Zr), La, Ce, Nd, Sm, Pr, Er, Gd, Eu, Tb, Dy, and Yb; Al, Si glass (for La, Ce, Nd, Sm, Pr, Er, Gd, Eu, Tb, Dy, and Yb), and crocoite (for Pb) were used.

Geological setting

Field geology

Metavolcanics and metasediments are the oldest rock units in the El-Sibai area of granitic rocks. These rocks are intruded by a granitic intrusion of

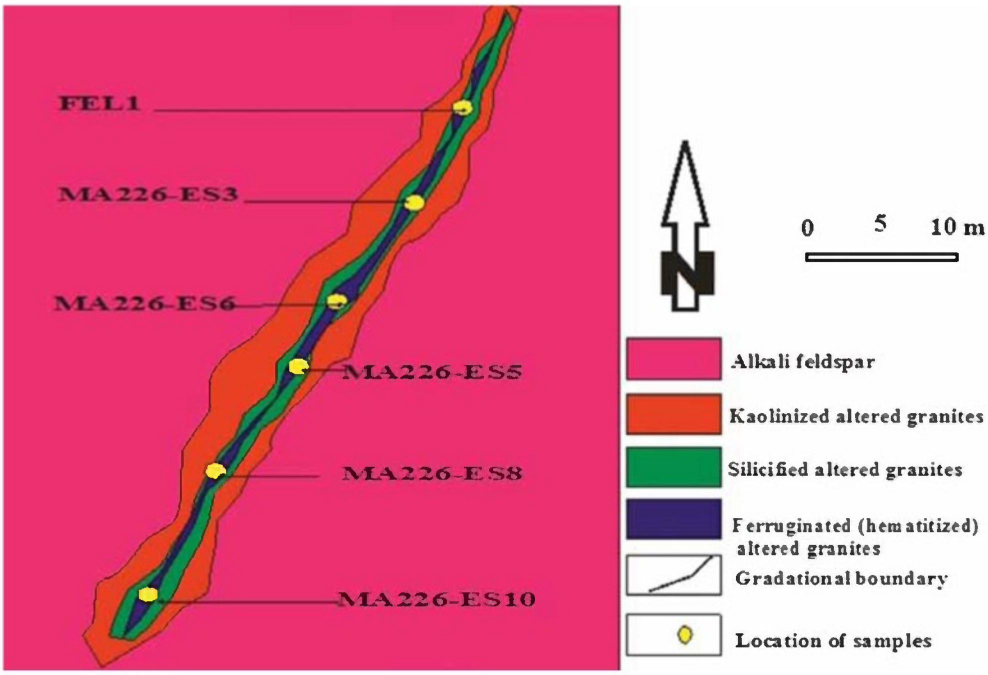

Fig. 2. Sketch of the different types of altered granites in El-Sibai shear zone, Central Eastern Desert, Egypt.

Gabal El-Sibai and Gabal Abu El-Tiyur. Younger granites of El-Sibai and Abu-Tiyur plutons are intruded in the metasediments, metavolcanics and several xenoliths from these older rocks of different sizes and shapes. They are pink in color and characterized by exfoliation and cavernous weathering. These granites are characterized by the presence of pegmatite pockets composed of feldspars, quartz and mica. All rock units are dissected by numerous mafic (basalt and dolerite) and alkaline bostonite dykes, which mainly follow the NW-SE direction. A NNE-SSW and N-S sets of faults cut the granitic pluton. These faults are mainly of strike-slip type (sinistral) and vary in length from 1.5 to 4 km.

A shear zone trending NNE-SSW dissects the northern segment of Gabal El-Sibai (1484 m.a.s.l) and extends for 3 km. The granite becomes mylonitized and cataclased within the shear zone. The identification of this shear zone was based on landsat images and field observations. The intensely exposed mineralized part of the shear zone varies in width from 0.5 to 3 m and in length from 300 to 500 m and is encountered at the alkali feldspar granite (Fig. 2).

Ferrugination, silicification and kaolinitization with few dark patches of manganese dendrites are the main wall rock alteration features observed within the investigated shear zone. These alterations are more pronounced in the granitic rocks on both sides of the shear zone (Fig. 3a). Deep reddish brown color mostly characterizes the strongly ferruginated rocks, while the lighter creamy and brownish yellow tones could be attributed to the weathering of feldspars by kaolinitization process. The silicified granite is characterized by its hardness and lighter rosy tones. Sheared and altered zones are suitable for circulating hydrothermal solutions and present favourable sites for the rare-metal mineralizations.

Petrography

Fresh surfaces of El-Sibai peralkaline granites are medium-to coarse-grained and consist essentially of perthites, quartz, oligoclase, microcline, biotite, minor amount of alkali amphiboles and alkali pyroxenes. Zircon, fluorite, apatite, monazite, allanite and hematite are the main accessory minerals. They are usually of hypidiomorphic granular texture. The microcline perthites may dominate strongly over orthoclase perthites. Quartz occurs as anhedral crystals. A graphic texture has been observed in few samples, i.e quartz intergrowth with K-feldspar. Plagioclase occurs as albite and is less abundant than perthites. It occurs as small interstitial crystals between quartz, perthites and riebeckite. Alkali pyroxene occurs as aegirin and is characterized by the presence of zircon, fluorite, apatite, allanite and monazite, which appear as inclusions. Alkali amphiboles occur as riebeckite and arfvedsonite, showing weak pleochroism from blue to deep blue.

All constituents of altered granites from the shear zone show cataclastic effects and have corroded edges. Quartz (30-45 %) sometimes shows clear signs of mylonitization and annealing. Brecciation took place prior to and/or is contemporaneous with the hydrothermal solutions. K-feldspars are represented by string type perthite with subordinate microcline. They are penetrated by relatively fine-grained veinlets of quartz and are kaolinized along the cleavage planes and fractures (Fig. 3 b, c). The cracks are filled with iron oxides which are originated from the hydrothermal solutions (Fig. 3 d). Cataclased albite (10 %) is commonly altered to sericite and its abundance increases in the mineralized samples. Cataclasis produced microfaults in the crystals and bending of the twin lamellae. Iron oxides are observed within all investigated thin sections either as a primary phase or as a secondary phase resulting from the alteration of other primary minerals, which are completely replaced by hematite (Fig. 3 e, f). Sometimes the original composition of the granites is obscured and becomes difficult to be determined due to the high intensity of ferrugination.

Thorite appears in two forms; in euhedral to subhedral crystals, and as long acicular radiating aggregates associated with iron oxide and zircon (Fig. 3 d), displaying bright yellow and blue interference colours. Accessory minerals are mainly metamictic zircon, monazite, rutile, fluorite, xenotime and opaque minerals. Zircon is in an optical microscope light gray and surrounded by hematite (Fig. 4 a, b), while the thorite occurs as lighter gray long acicular

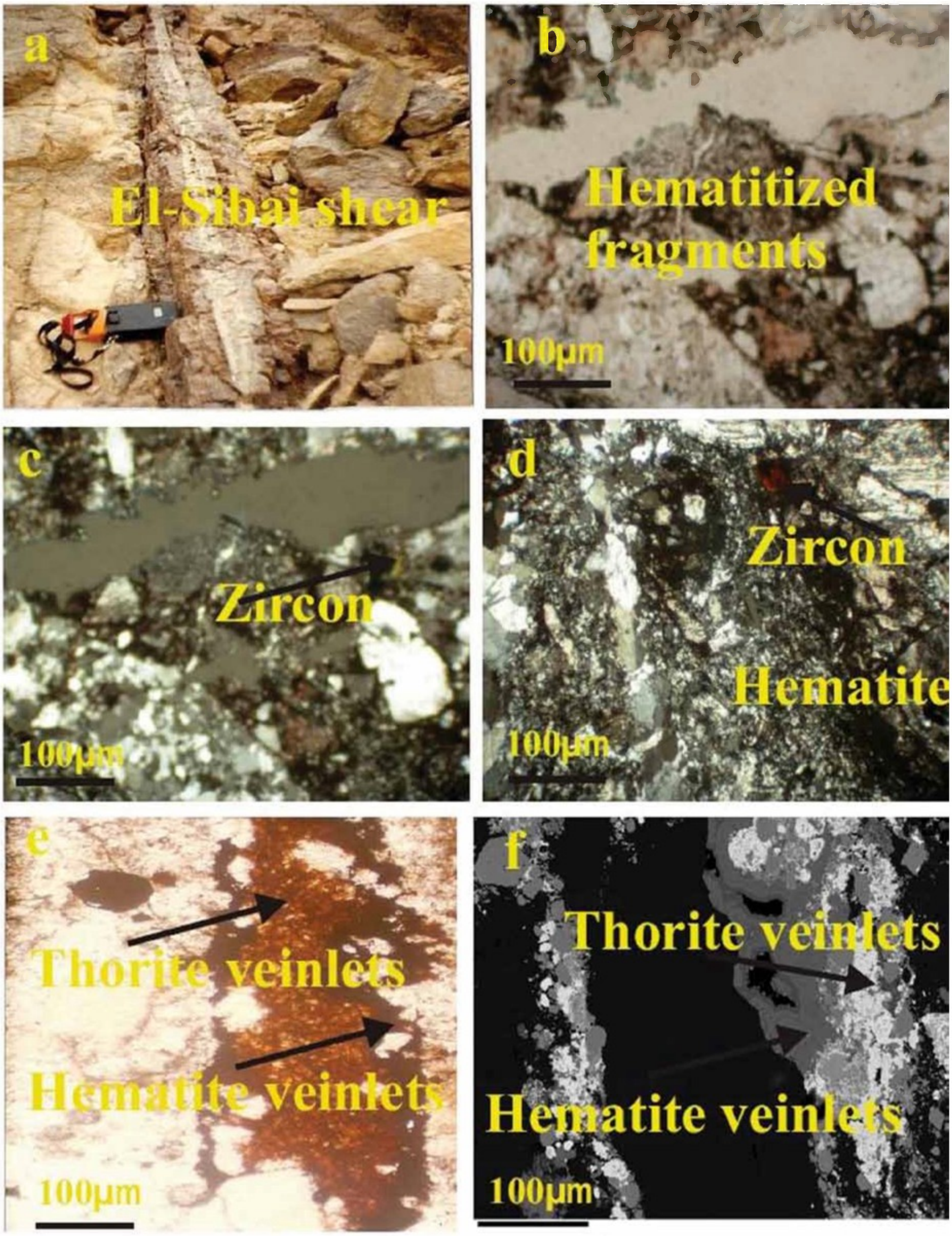

Fig. 3. a) NNE trending of peralkaline granite in El-Sibai shear zone, b) Average mineral composition of cataclastic and mylonite rocks within the El-Sibai shear zone, parallel nicoles and c) crossed nicols, d) Photomicrograph of large crystals of zircon associated with irone oxides (hematite) within the El-Sibai shear zone, e) Photomicrograph of mineralized veinlets of thorite associated with hematite, and f) its corresponding BSE image.

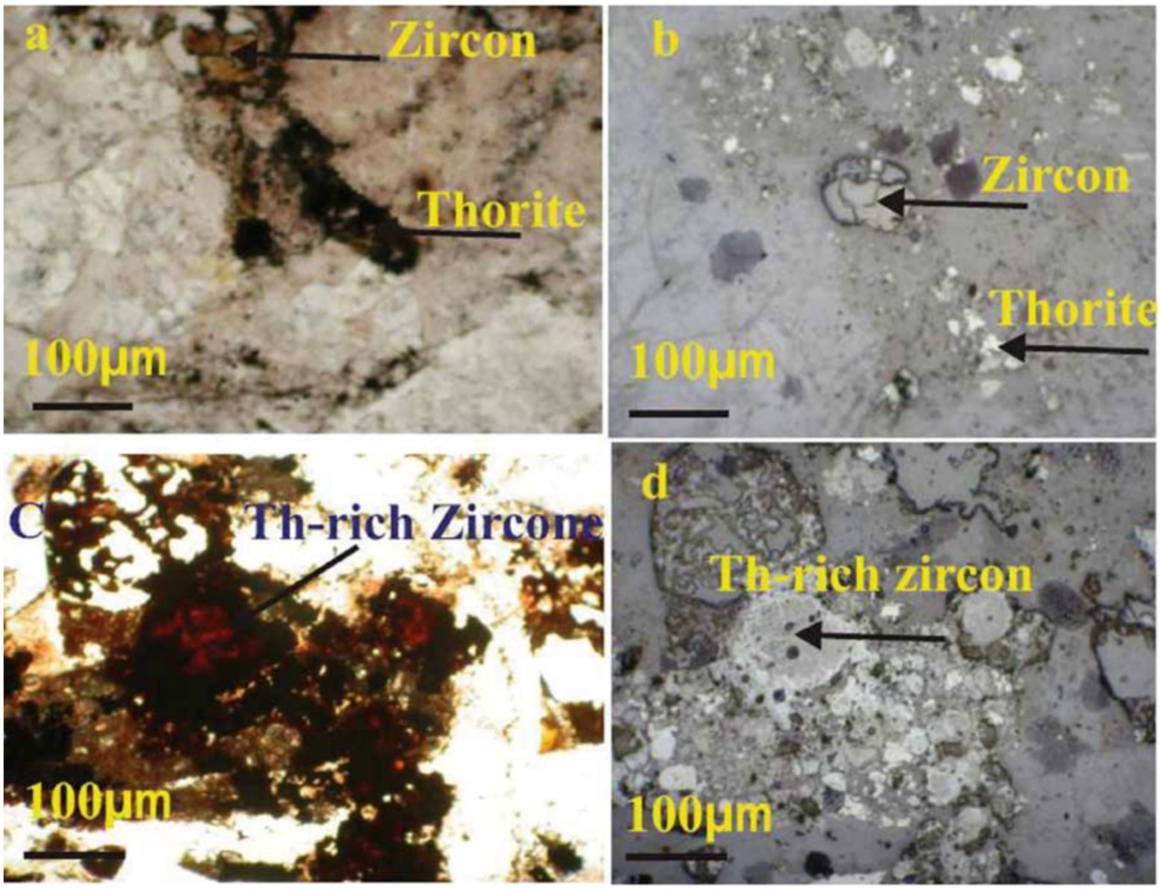

Fig. 4. a) Photomicrograph of zircon and thorite, polarized light b) The same as previous photograph under crossed nicols, c) Photomicrograph of large zircon crystals surrounded by thorite minerals in parallel nicols, and d) under crossed nicols.

radiating aggregates associated with hematite and display reddish brown, yellowish brown and dark brown interference colours (Fig. 4 c, d).

Mineralogy

Detailed mineralogical investigated of columbite–tantalite, Th- and U-Nb, zircon and Th-rich zircon minerals in the mineralized peralkaline granites of El-Sibai shear zone, revealed the presence of primary Th (thorite, huttonite monazite and Th-rich zircon), and U-Nb (plumbopyrochlore), zirconolite (Nb-Zr), zircon (Hf), monazite, fluorite, and fluorapatite. Optical microscopy, SEM, and EPMA were used to characterize ferrocolumbite, pyrochlore and plumbopyrochlore, primary Th (thorite, and huttonite), zirconolite (mixture of zircon and columbite), zircon (Hf), Th-rich zircon, monazite, fluorite, fluorapatite, and cerite-(Ce). A brief description of accessory heavy minerals in this study of rare-metal peralkaline granites are as follows:

Columbite group AB_2O_6

The Columbite group of minerals comprises a large number of structurally related orthorhombic AB_2O_6 coumpounds. The Columbite subgroup is Nb-dominant, and the Ta- subgroup Ta dominant. Most commonly occurring as accessory minerals in granite pegmatites (Gaines et al., 1997), columbite-group minerals contain U (and Th) in various amounts and are commonly metamict, but there is no description with U as an essential constituent. The relatively small octahedral A site is commonly occupied by Mg^{2+} (magnesiocolumbite) and transition-metal cations, such as Fe^{2+} (ferrocolumbite) and Mn^{2+} (manganocolumbite), U and Th substitutions are relatively rare.

Nb and Ta form mostly complex oxides or hydroxides, they appear rarely as silicates in different rock types. This series represents solid solution between columbite (Fe, Mn)$(Nb,Ta)_2O_6$ and tantalite (Fe, Mn)$(Ta,Nb)_2O_6$. In fact, similarity between Nb and Ta elements, both being pentavalent, preferring octahedral coordination in oxide compounds with similar ionic radii=0.72 Å (Whittaker & Muntus, 1970), cause extensive mutual substitution between them. The columbite-tantalite series are the most abundant in granites and pegmatites, particularly those containing albite and Li silicates associated with albite, microcline, lepidolite, and muscovite. Columbite is frequently considered to be a carrier of U-Th and REE. In many cases, its radioactivity is related to minute inclusions of radioactive minerals, surrounded by conspicuous radioactive halos.

A large number of complex Nb, Ta, and Ti oxides are known to contain U in various amounts. These minerals mostly occur as accessory minerals in granitic rocks and granitic pegmatites. There are several important Nb and Ta ore minerals, which may be mined for REEs. A few of them contain U as an essential constituent, which is usually oxidied to a certain degree (Smith, 1984). Nearly all contain some U and Th in solid solution, and are therefore important actinide hosts in granitic rocks, as well as important source for dissolved U in the hydrothermal and meteoric waters with which they interact. Many of these minerals are commonly metamict; due to their abilities to incorporate radioactive elements, they can also be strongly altered.

Metamict minerals offer a special challenge to mineralogists trying to obtain structural information about their crystalline precursors. Redox conditions during annealing may change oxidation states of some elements (e.g. Fe or U). Due to possible post-formation alteration, it is not al-

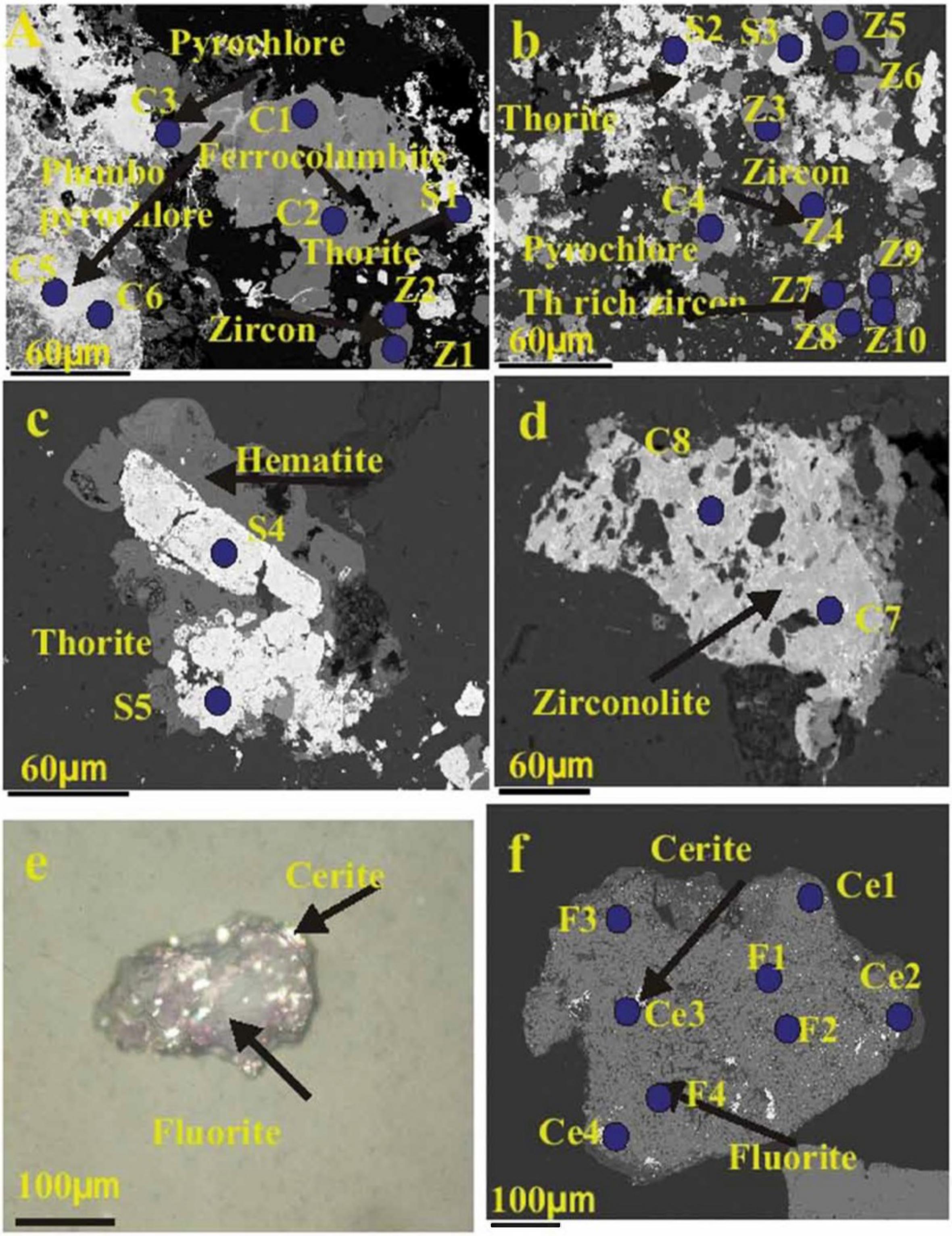

Fig. 5. a) pyrochlore and plumbopyrochlore associated with thorite and zircon in the El-Sibai shear zone, BSE image b) Thorite associated with euhedral crystals of zircon, BSE image c) large euhedral thorite with hematite, BSE image d) large crystal of zirconolite, and BSE image e) photomicrograph of violet fluorite with cerite inclusions, polarized light and f) its corresponding BSE image for the same crystal.

ways clear what was the oxidation state of some elements at the time of crystallization (Warner & Ewing, 1993). According to their structure these minerals are divided into ixiolite, samarskite (wolframite) and columbite groups. They consist of approximately hexagonal close packed O atoms. The A and B sites are octahedrally coordinated. Octahedra share edges to form chains along [001] and layers parallel to [100] (notation after Warner & Ewing, 1993). All three groups have structures that derivates of the α-PbO_2 structure (Warner & Ewing, 1993). The structures of pyrochlore and zirconolite share some basic features with those of fergusonite and aeschynite, namely octahedral chains and large A sites; however, the pyrochlore structure is a derivative of the CaF_2 structure (Chakoumakos, 1984) and zirconolite is a derivative of the pyrochlore structure (Bayliss et al., 1989). The most important U-bearing Nb-Ta-Ti oxides are discussed further below.

Ferrocolumbite [$(Fe, Mn)(Nb,Ta)_2O_6$] crystals that occur in the El-Sibai shear zone are generally dark grey to black when observed in the microscope. They are present in the form of subhedral to anhedral crystals and range in size from 30 to 100 μm (Fig. 5a, b). The EPMA of the minerals revealed that the major elements in ferrocolumbite at A sites are FeO (16.52 wt%) and MnO (4.57 wt%), and at B sites Nb_2O_5 (74.68 wt%), and Ta_2O_5 (2.61 wt%). Also, minor amounts of Ti, Th, U, Y and LREE were reported as substitutions in ferrocolumbite (Fig. 5a, Table 1).

Pyrochlore group [$A_{1-2}B_2O_6(O,OH,F)$]

This group is particularly important group with Nb-Ta-Ti oxides that contain substantial U. The structure of ideal pyrochlore group, is a derivative of the fluorite structure (Chakoumakos, 1984, 1986). The structure with Ta, Nd, and Ti, and which can also contain Fe, Sn, W, and Sb (Mandarino, 1999); Sb^{5+} can even dominate at the B site, as in the case of roméite (Brugger et al., 1997). The A site is eight coordinated (distorted cube) and may contain alkalis, alkaline earths, REE and actinides. In pyrochlore charge balance is maintained through cation substitutions at either A or B sites as well as throught anionic substitutions. Three pyrochlore subgroups are distinguished in accordance with the predominant cation in the B sites. Niobium prevail over Ta in the pyrochlore subgroup, whereas Ta exceeds Nb in the microlite subgroup. Both pyrochlore and microlite subgroups have (Ta+Nb)>2Ti, whereas the betafite subgroup is characterized by 2Ti>(Ta+Nb). U substitutions at the A sites and metamict pyrochlore are common. Although virtually all these minerals contains some U, only uranmicrolite and uranopyrochlore of pyrochlore group contain U as an essential constituent (Lumpkin & Ewing, 1995).

Pyrochlore [$(Fe, Mn)(Nb, Ta, Ti)_2O_6(O,OH,F$] occurs as subhedral to anhedral crystals in the El-Sibai altered peralkaine granites, and range in size from 5 to 10 μm (Fig. 5a, b). Its radioactivity is related to minute inclusions of radioactive minerals. The EPMA of the crystals showed that the major elements in pyrochlore are FeO (15.89 wt%) and MnO (4.57 wt%) at A sites, and Nb_2O_5 (65.94 wt%), Ta_2O_5 (3.2 wt%) and TiO_2 at B sites. Also minor amounts of U, Th, Y, and LREE were reported as substitutions in pyrochlore (Fig. 5a,b, Table 1).

Plumbopyrochlore [$(Pb,U,Ca)_{2-x}Nb_2O_6(OH)$] was found only in the El-Sibai shear zone as an alteration phase, containing potential concentrations of the high-field-strength elements (HFSE), such as Ti, Nb, and Ta, besides U. The EPMA of the sample MA226ES10-C5 revealed that the major elements in plumbopyrochlore are at A sites PbO (30.57 wt%), UO_2 (7.26 wt%), FeO (11.93 wt%), CaO (1.7 wt%) and MnO (0.26 wt%), and at B sites Nb_2O_5 (31.65 wt%), TiO_2 (5.81 %) and Ta_2O_5 (2.50 wt%), (Fig. 5 a, b; Table 1).

Zirconolite group ($A_2B_2O_7$)

The structure of zirconolite [$(Ca,Fe)(Zr,U)Ti_2O_7$] can be described as a derivative of the pyrochlore structure, with octahedrally coordinated B sites and A sites in distorted cubes. Zirconolite is monoclinic and has two distinct A sites, designated as A (Ca) and A' (Zr). Zirconolite is Ti dominant at the B site, Nb- dominant zirconolite minerals were identified from carbonatite in Kovdor (Williams & Gieré, 1996); however, no Ta- dominant zirconolite-group minerals are known. As for most other Ta-Nb-Ti oxides, U substitutes at the large cation sites primarily for Ca at the A site in zirconolite; no U dominant zirconolite-group minerals are known. Nevertheless, U and Th substitutions in zirconolite can induce substantial structural change, consequently the metamict zirconolite are not rare. As an important accessory mineral in large variety of rocks, zirconolite has also been studied as a potential actinide-bearing nuclear waste form (Lumpkin et al., 1994). It is as an alteration phase between columbite and zircon with size range from 20 to 50 μm (Fig. 5d). The EPMA of the sample MA226E8-C8 reflect the major elements in zirconolite are at A sites ZrO_2 (26.25 wt%), SiO_2 (18.97 wt%), FeO (13.21 wt%), and CaO (1.01 wt%), and at B sites Nb_2O_5 (10.99 wt%), TiO_2 (3.94 wt%), UO_2 (1.1 wt%), ThO_2 (8.79 wt%), Y_2O_3 (6.48 wt%), and Ta_2O_5 (0.2 wt%). Also small amounts of LREE (1.2 wt%) were reported as substitutions at B sites of zirconolite (Fig. 5d, Table 1).

Thorium mineralizations

In the El-Sibai altered granites (shear zone) two mineral species of Th-minerals, namely thorite and huttonite monazite are found. Under reducing conditions, U transport is likely to be measured in fractions of a centimeter, although F and Cl complexes can stabilize U (IV) within the solution (Keppler & Wyllie, 1990). If there is sufficient concentration of oxygen to stabilize the uranyl ion, UO^{2+} and its complexes, U can migrate many kilometers from its source to precipitate U-bearing minerals (plumbopyrochlore and zirconolite).

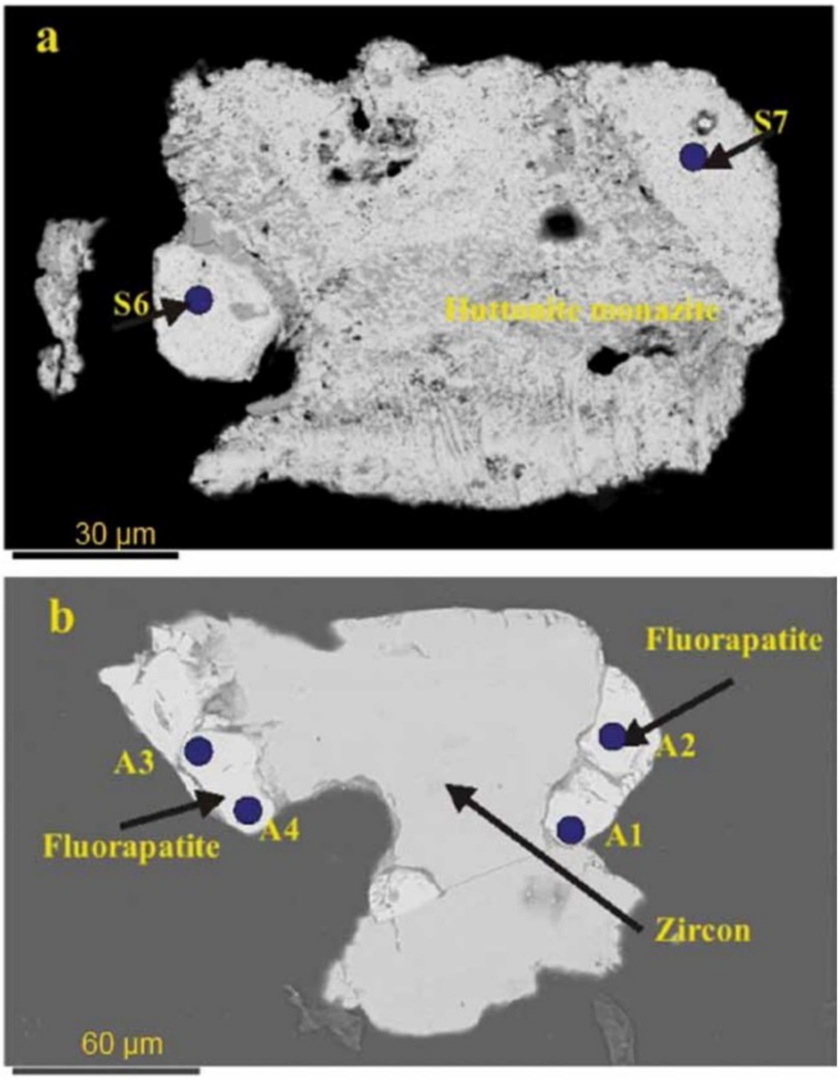

Fig. 6. SEM-BSE images a) huttonite after monazite, and b) fluorapatite cystals associated with zircon and titanite.

Thorite [Th,U(SiO_4)] exihibits euhedral to subhedral crystals in the El-Sibai altered peralkaline granites of the investigated area. Thorite is black to brown and shows varying degrees of alteration. It somewhat resembles zircon, occurring as small, square prismatic crystals with pyramidal points and has been found around the zircon crystals as yellowish brown phases (Fig. 5b, c). The chemical composition of thorite is given in Table 2. ThO_2 ranges from 68.13 to 78.64 wt% (mean 73.48 wt%), UO_2 ranges from 0.838 to 1.54 wt% (mean 1.07 wt%), SiO_2 ranges from 12.97 to 14.38 wt% (mean 13.71 wt%), Y_2O_3 (3.45 wt%), and FeO (3.22 wt%). Small amounts of Ca, P and LREE were reported as substitutions in thorite (Fig. 5b, c; Table 2).

Huttonite monazite [(Th,U,LREE)PO_4] occurs as as an alteration phase between thorite and monazite, and range in size from 30 to 100 µm (Fig. 5d). The EMPA of these crystals reflect the huttonite composition (Table 2). These results indicate that the mean values of major elements in huttonite monazite are ThO_2 (61.06 wt%), P_2O_5 (12.90 wt%), Al_2O_3 (1.11 wt%), CaO (4.75 wt%), Ce_2O_3 (11.80 wt%), Y_2O_3 (1.29 wt%), and U (0.7 wt%). Very small amounts of Si and LREE were reported as substitutions in huttonite (Fig. 6a, Table 2). According to Frondel and Cuttito (1955) huttonite and thorite are formed at hydrothermal conditions over a temperature range 300 °C to 700 °C. The formation of huttonite is favoured by alkaline conditions and thorite by acid conditions.

Accessory minerals

Accessory minerals include zircon, fluorite, monazite, and cerite-(Ce); among sulfides and hydroxides pyrite and hematite prevail.

Zircon ($ZrSiO_4$) is a common accessory mineral in plutonic igneous rocks. It is generally found as small inclusions in minerals, however in granites and pegmatites it can form large well developed crystals (Deer et al., 1966). Hussein (1978) and Abadalla et al. (2008) stated that the radioactive zircons are usually zoned and are characterized by metamictization. The explanation for the origin of the "metamict state" is that the internal order of the originally crystalline form has been destroyed by $\propto$-particles bombardment from radionuclides within the structure. It is partially or completely modified giving amorphous zircon a more isotropic character; i.e, metamict zircon. Zircon crystals in the studied mineralized granites are mainly characterized by considerable metamictization due to thorium and uranium inclusions.

Zircon occurs as pale to deep brown euhedral prismatic grains and is generally sub-translucent to opaque with dull luster. The most common habit is the bipyramidal form with various pyramidal faces (Fig. 4a, b). However, some zircon crystals are characterized by extremely short prisms and are more or less equidimensional, exhibiting square cross section. Zircon occurs as euhedral to subhedral prismatic (six-or eight-sided), 20 to 150 µm zoned crystals, which contain clusters of inclusions of radioactive minerals. The core of zircon in the El-Sibai shear zone contains high Hf contents, in contract to the rim with low Hf contents (Table 3). Both varieties of zircon, unaltered and altered zircon (Th-rich zircon), have been recognized in the El-Sibai altered granites (shear zone). The chemical composition of zircon is presented in Table 3. Th-rich zircon has higher ThO_2 and UO_2, and lower ZrO_2 and SiO_2, in comparison to unaltered zircon. Generally, domains of altered zircon (Th-rich zircon) are characterized by greater enrichment in CaO, FeO, P_2O_5, HfO_2 and Al_2O_3 than unaltered domains (Fig. 5b, Table 4). Similar results were observed by Förster (2000, 2006) and Abd El-Naby (2009), who reported on

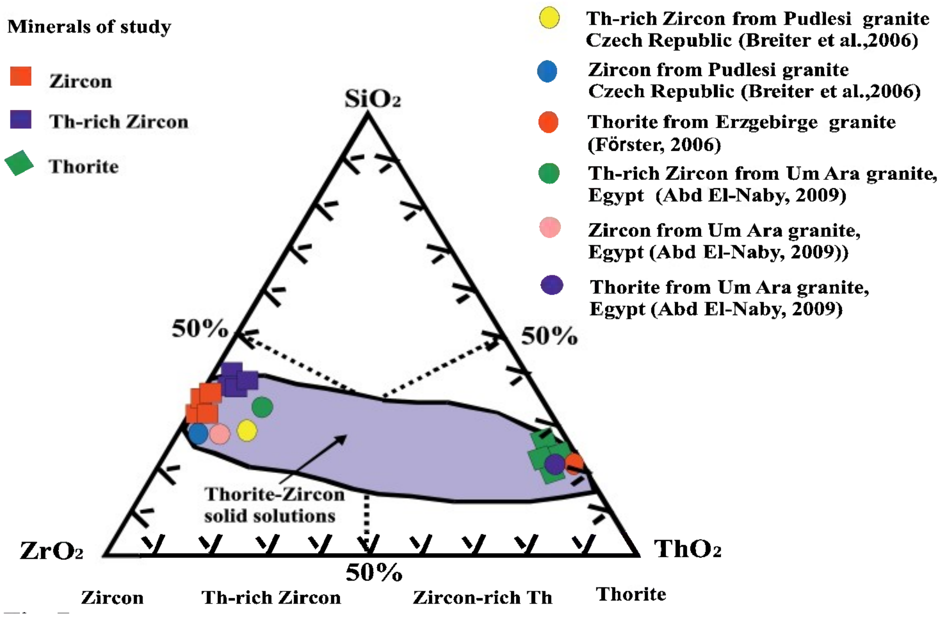

Fig. 7. Composition of thorite and zircon plotted on the basis of SiO_2–ThO_2–ZrO_2. The shaded field encloses the composition of thorite-zircon solid solution. See also Breiter et al. 2006, Fröster et al., 2006, and Abd El-Naby, 2009.

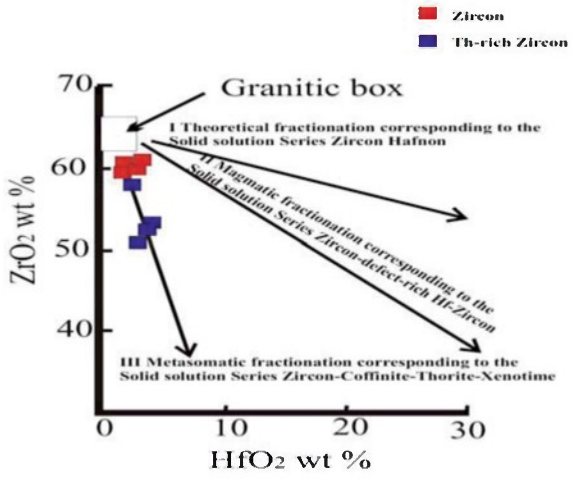

Fig. 8. ZrO2 versus HfO_2 diagram of zircons from rare metal granitoids, Eastern Desert, Egypt. The shown trends are modified from Kempe et al. (1997) and Abadalla et al. (2008). The granite box, comprising Zr-Hf ranges in granites from Wedepohl (1978).

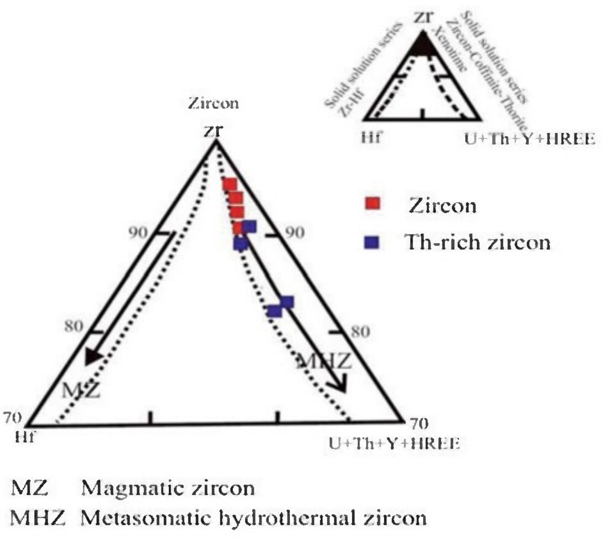

Fig. 9. Zr-Hf-(Y+ U+ Th +HREE) ternary diagram for zircon compositions in rare metal granitoids, Eastern Desert, Egypt, the dashed line represents an interpretative boundary that limits the compositional gap between the two zircon series. The shown trends of magmatic zircon (MZ) and metasomatic hydrothermal zircon (MHZ) are drawn by Abadalla et al. (2008).

Table 1. Mineral chemistry of selected some minerals from El-Sibai shear zone, the minerals obtained by EMPA, the major oxides by (wt%).

Rock	**El-Sibai**	**El-Sibai**	**El-Sibai**	**El-Sibai**	**El-Sibai**	**El-Sibai**	**El-Sibai**	**El-Sibai**
Sample	**MA226 ES10-C1**	**MA226 ES10-C2**	**MA226 ES10-C3**	**MA226 ES6-C4**	**MA226 ES10-C5**	**MA226 ES10-C6**	**MA226 ES10-C7**	**MA226 ES8-C8**
Mineral name	**Ferro-columbite**	**Ferro-columbite**	**Pyrochlore**	**Pyrochlore**	**Plumbo-pyrochlore**	**Plumbo-pyrochlore**	**Zirconolite**	**Zirconolite**
SiO_2	0.110	0.109	1.119	1.190	3.15	4.65	18.13	18.97
Na_2O	0.033	0.033	0.143	0.152	1.333	1.228	0.090	0.104
K_2O	0.000	0.000	0.000	0.000	0.033	0.030	0.000	0.000
ZrO_2	0.000	0.000	0.245	0.286	0.216	0.198	25.28	26.25
HfO_2	0.041	0.041	0.000	0.000	0.003	0.000	1.198	1.385
P_2O_5	0.032	0.031	0.030	0.032	0.086	0.079	0.281	0.325
CaO	0.047	0.046	2.106	2.240	1.705	1.570	0.047	1.013
FeO	16.52	16.38	14.91	15.89	11.93	10.98	12.28	13.21
TiO_2	1.511	1.498	5.95	6.34	5.81	5.35	3.41	3.94
MnO	4.57	4.53	1.093	1.165	0.289	0.266	0.104	0.120
Y_2O_3	0.329	0.326	0.852	0.908	0.287	0.264	5.60	6.48
Ce_2O_3	0.000	0.000	0.099	0.106	0.756	0.696	0.760	0.879
La_2O_3	0.004	0.004	0.000	0.000	0.219	0.201	0.137	0.159
Pr_2O_3	0.000	0.000	0.000	0.000	0.036	0.033	0.093	0.108
Nd_2O_3	0.074	0.073	0.000	0.000	0.042	0.038	0.069	0.079
Gd_2O_3	0.000	0.000	0.060	0.064	0.190	0.175	0.000	0.000
SnO_2	0.114	0.113	0.245	0.261	0.028	0.026	0.000	0.000
Nb_2O_5	74.68	74.03	61.87	65.94	31.65	29.14	9.50	10.99
Ta_2O_5	2.613	2.591	2.999	3.20	2.503	2.384	0.172	0.199
PbO	0.000	0.000	0.000	0.000	30.57	28.14	0.000	0.000
ThO_2	0.085	0.084	1.399	1.480	1.027	0.946	7.60	8.79
UO_2	0.111	0.110	0.688	0.733	7.26	6.68	0.868	1.104
Total	100.87	99.96	93.81	99.98	99.11	93.07	86.45	94.10
Structural formula for 4 oxygen atoms								
Si	0.003	0.003	0.035	0.037	0.158	0.145	0.567	0.655
Na	0.001	0.001	0.005	0.005	0.042	0.038	0.003	0.003
K	0.000	0.000	0.000	0.000	0.001	0.001	0.000	0.000
Zr	0.000	0.000	0.008	0.009	0.007	0.006	0.790	0.914
Hf	0.001	0.001	0.000	0.000	0.000	0.000	0.016	0.019
P	0.001	0.001	0.001	0.001	0.002	0.002	0.007	0.008
Ca	0.001	0.001	0.059	0.062	0.047	0.044	0.001	0.028
Fe	0.516	0.512	0.466	0.497	0.373	0.343	0.384	0.444
Ti	0.047	0.047	0.186	0.198	0.182	0.167	0.107	0.123
Mn	0.143	0.142	0.034	0.036	0.009	0.008	0.003	0.004
Y	0.007	0.007	0.018	0.019	0.006	0.006	0.117	0.135
Ce	0.000	0.000	0.002	0.002	0.016	0.015	0.016	0.018
La	0.000	0.000	0.000	0.000	0.005	0.004	0.003	0.003
Pr	0.000	0.000	0.000	0.000	0.001	0.001	0.002	0.002
Nd	0.002	0.002	0.000	0.000	0.001	0.001	0.001	0.002
Sn	0.001	0.001	0.003	0.003	0.001	0.001	0.000	0.000
Nb	1.167	1.157	0.967	1.030	0.495	0.455	0.148	0.172
Ta	0.025	0.025	0.029	0.031	0.014	0.013	0.002	0.002
Th	0.003	0.028	0.046	0.049	0.034	0.031	0.249	0.288
U	0.004	0.003	0.022	0.035	0.227	0.209	0.027	0.035
Nb / Ta	28.58	28.58	20.66	20.61	21.10	21.06	55.10	55.12
Th / U	0.76	0.76	2.03	1.34	0.14	0.14	8.76	7.96

chemical analyses of zircon, thorite, and Th-rich zircon (Fig. 7). Despite the incorporation of some oxides (e.g. CaO, FeO, P_2O_5, HfO_2 and Al_2O_3) and a hydrous component, the majority of domains of both zircon varieties maintain a constant SiO_2/ZrO_2 ratio (Table 4).

The EMPA for these crystals reflect the zircon composition (Table 3). This indicates that the major elements in zircon are ZrO_2 (60.44 wt%), SiO_2 (31.94 wt%), HfO_2 (2.94 %), and Yb_2O_3 (0.5 wt%) with significant amounts of ThO_2 (0.36 wt%), UO_2 (0.16 wt%), FeO (0.82 wt%), and Y_2O_3 (0.4 wt%). In contrast, the EPMA of the Th-rich zircon showed in average mainly ZrO_2 (53.47 wt%), SiO_2 (29.55 wt%), HfO_2 (3.34 wt%), and Yb_2O_3 (0.56 wt%) with significant amounts of ThO_2 (5.46 wt%), UO_2 (0.55 wt%), FeO (0.85 wt%), and Y_2O_3 (2.16 wt%) composed of Th-rich zircon (Table 4).

Petrogenesis of zircon

Kempe et al. (1997) and Abadalla et al. (2008) considered that both magmatic and metasomatic mechanisms or their combination were responsible for yielding extreme Zr/Hf fractionation and hence the formation of Hf-rich zircon. The aforementioned petrographical and geochemical characterization of metasomatically and magmatically specialized rare metal granitoids, has greatly contributed to clear discrimination of Zr/Hf fractionation in the two main associations (i.e. magmatic & metasomatic).

The zircon of the investigated rare metal El-Sibai altered granite frequently contains hafnium in amounts ranging between 2.14 and 4.23 wt%, therefore the nomenclature scheme of Correia Neves et al. (1974) for the isomorphous zircon ($ZrSiO_4$)–Hafnon ($HfSiO_4$) series has been used to designate it. The term #Hf denotes the hafnon end-member ($HfSiO_4$) mole% or more precisely, the atomic ratio: 100*Hf/(Zr + Hf) (Table 3). Zircon has #Hf = 0–10; hafnian zircon #Hf = 10–50; zirconian hafnon #Hf = 50–90 and Hafnon #Hf = 90–100.

However, in the present study zircon with enhanced Hf content (i.e. #Hf = 3–10) was designated as Hf-rich zircon in order to distinguish it from zircon with very low #Hf. Zircon of El-Sibai peralkaline granite is characterized by a primitive composition with respect to the content of Hf, Y, U, Th, and HREE (Figs. 8, 9; Table 3). Its ranging between 3.54 and 6.44 and thus, it can be designated as a normal zircon according to the scheme

Table 2. Mineral chemistry of selected some minerals from El-Sibai shear zone, the minerals obtained by EMPA, the major oxides by (wt%).

Rocks	**El-Sibai**	**El-Sibai**	**El-Sibai**	**El-Sibai**	**El-Sibai**	**El-Sibai**	**El-Sibai**	**El-Sibai**	**El-Sibai**
Sample	**MA226 ES10-S1**	**MA226 ES10-S2**	**MA226 ES5-S3**	**MA226 ES6-S4**	**MA226 ES3-S5**	**Average N=5**	**MA226 ES3-S6**	**MA226 ES3-S7**	**Average N=2**
Minerals	**Thorite**	**Thorite**	**Thorite**	**Thorite**	**Thorite**		**Huttonite monazite**	**Huttonite monazite**	
Al_2O_3	0.000	0.000	0.000	0.000	0.000	0.000	1.116	1.103	1.11
SiO_2	14.38	14.06	13.86	13.29	12.97	13.71	0.357	0.365	0.361
Na_2O	0.101	0.084	0.016	0.079	0.015	0.059	0.000	0.000	0.000
K_2O	0.113	0.048	0.000	0.045	0.000	0.069	0.000	0.000	0.000
ZrO_2	0.567	1.178	0.206	1.114	0.193	0.652	0.077	0.079	0.078
HfO_2	0.032	0.083	0.000	0.078	0.000	0.064	0.169	0.173	0.171
P_2O_5	0.201	0.269	0.254	0.254	0.238	0.243	12.74	13.05	12.90
CaO	0.328	0.260	0.742	0.245	0.694	0.454	4.69	4.80	4.75
FeO	1.062	0.350	7.43	0.330	6.95	3.22	1.01	0.985	0.998
MnO	0.077	0.026	0.009	0.024	0.009	0.029	0.000	0.000	0.000
Y_2O_3	3.38	3.63	3.51	3.43	3.29	3.45	1.289	1.296	1.293
Ce_2O_3	0.036	0.000	0.000	0.000	0.000	0.036	11.10	12.5	11.80
Pr_2O_3	0.145	0.000	0.000	0.000	0.000	0.145	0.000	0.000	0.000
La_2O_3	0.033	0.000	0.000	0.000	0.000	0.033	0.000	0.000	0.000
Nd_2O_3	0.066	0.000	0.000	0.000	0.000	0.066	1.595	1.634	1.615
Eu_2O	0.000	0.000	0.000	0.000	0.000	0.000	0.231	0.236	0.234
Gd_2O_3	.1500	0.075	0.000	0.071	0.000	0.076	0.907	0.929	0.918
Dy_2O_3	0.000	0.000	0.000	0.000	0.000	0.000	0.24	0.246	0.245
HO_2O_3	0.000	0.000	0.000	0.000	0.000	0.000	0.133	0.137	0.135
Er_2O_3	0.000	0.000	0.000	0.000	0.000	0.000	0.250	0.240	0.245
Yb_2O_3	0.000	0.000	0.000	0.000	0.000	0.000	0.022	0.023	0.023
Nb_2O_5	0.346	0.405	0.069	0.383	0.064	0.253	0.000	0.000	0.000
Ta_2O_5	0.043	0.000	0.000	0.000	0.000	0.043	0.000	0.000	0.000

Table 2. (continued)

PbO	0.000	0.000	0.000	0.000	0.000	0.000	0.111	0.114	0.112
ThO_2	73.49	78.64	72.81	74.32	68.13	73.48	60.69	61.43	61.06
UO_2	1.543	0.886	1.086	0.838	1.016	1.074	0.693	0.710	0.702
Total	96.09	99.98	100.01	94.51	93.57	96.83	98.60	99.95	99.28
Structural formula on basis of 4 oxygen atoms									
Al	0.000	0.000	0.000	0.000	0.000	0.000	0.023	0.023	0.023
Si	0.444	0.434	0.428	0.410	0.400	0.420	0.011	0.011	0.011
Na	0.003	0.003	0.001	0.003	0.001	0.002	0.000	0.000	0.000
K	0.003	0.001	0.000	0.001	0.000	0.002	0.000	0.000	0.000
Zr	0.018	0.037	0.006	0.035	0.006	0.020	0.001	0.001	0.001
Hf	0.001	0.001	0.000	0.001	0.000	0.001	0.002	0.002	0.002
P	0.005	0.007	0.006	0.006	0.006	0.006	0.319	0.326	0.323
Ca	0.009	0.007	0.021	0.007	0.012	0.013	0.130	0.133	0.131
Fe	0.030	0.010	0.206	0.009	0.193	0.090	0.032	0.031	0.032
Mn	0.002	0.001	0.001	0.001	0.000	0.002	0.000	0.000	0.000
Y	0.099	0.106	0.103	0.101	0.096	0.101	0.027	0.027	0.027
Ce	0.001	0.000	0.000	0.000	0.000	0.001	0.232	0.260	0246
Pr	0.004	0.000	0.000	0.000	0.000	0.004	0.000	0.000	0.000
La	0.001	0.000	0.000	0.000	0.000	0.001	0.000	0.000	0.000
Nd	0.002	0.000	0.000	0.000	0.000	0.002	0.033	0.034	0.034
Eu	0.000	0.000	0.000	0.000	0.000	0.000	0.005	0.005	0.005
Gd	0.005	0.001	0.000	0.002	0.000	0.003	0.019	0.019	0.019
Dy	0.000	0.000	0.000	0.000	0.000	0.000	0.005	0.005	0.005
Ho	0.000	0.000	0.000	0.000	0.000	0.000	0.003	0.003	0.003
Er	0.000	0.000	0.000	0.000	0.000	0.000	0.005	0.005	0.005
Yb	0.000	0.000	0.000	0.000	0.000	0.000	0.001	0.001	0.001
Nb	0.005	0.006	0.001	0.006	0.001	0.004	0.000	0.000	0.000
Pb	0.000	0.000	0.000	0.000	0.000	0.000	0.001	0.001	0.001
Th	1.341	1.435	1.329	1.356	1.243	1.34	1.108	1.121	1.115
U	0.026	0.015	0.019	0.014	0.017	0.018	0.012	0.12	0.012
Th / U	47.62	88.72	67.05	88.71	67.05	71.83	92.33	93.42	92.88
ΣA+B	2.0	2.07	2.11	1.96	1.98	2.02	1.98	2.01	2.00

N= number of samples

of Correia Neves et al. (1974). Zircon of the studied altered peralkaline granite zone is characterized by UO_2 and ThO_2 occur in high quantities in HREE (Figs. 8, 9; Table 3). Meanwhile Th-rich zircons of the hematitized and albitized granites are characterized by complex chemistry which is reflected in high to enhanced contents of Hf, U, Th, Y, HREE (Figs. 8, 9; Table 3) and therefore this zircon can be designated as Hf-rich zircon. The zoning terminology used here is based on the geochemical criteria given by Černý et al. (1985) for fractionated rare metal granitoids and pegmatites.

Fluorite CaF_2

Fluorite showed large blue to violet euhedral to subhedral crystals with a size range of 10-40 µm (Fig. 5e, f). The EPMA indicate that the major elements in fluorite are CaO (68.75 wt%) and F (45.83 wt%), with significant amounts of Ce_2O_3 (0.7 wt%), Y_2O_3 (2.7 wt%), UO_2 (0.02 wt%), ThO_2 (0.2 wt%) and REE (2 wt%) are reported as substitutions in fluorite (Table 5). Yttrium partially substitutes Ca. El-Kammar et al. (1997) concluded that the change in colour of fluorite is mainly controlled by the Y content. The presence of fluorite accompanying the mineralization indicates that the hydrothermal alteration processes were involved during shearing.

Cerite-(Ce) [Ce_9(Th, Ca) (Fe^{3+}, Mg) $(SiO_4)_6[SiO_3(OH)](OH)_3$]

The nomenclature of the REE minerals is unique, because names of simple end-members no longer exist. Since 1966 each mineral name consists of a structural formula name and the symbol of the dominant lanthanide element (Fleischer, 1987, 1989; Bayliss & Levinson, 1988). The crystal structures of many REE minerals are poorly-

Table 3. Mineral chemistry of selected some minerals from El-Sibai shear zone, the minerals obtained by EMPA, the major oxides by (wt%).

Rock	**El Sibai**	**El Sibai**	**El Sibai**	**El Sibai**	**El Sibai**	**El Sibai**	**El Sibai**
Sample	**Zircon Core MA226-E10 Z1**	**Zircon Rim MA226-E10 Z2**	**Zircon Core MA226-ES3 Z3**	**Zircon rim MA226-ES3 Z4**	**Zircon core FEL-2E4 Z5**	**Zircon rim FEL-2E4 Z6**	**Average N=6**
Al_2O_3	0.000	0.026	0.000	0.000	0.000	0.000	0.056
SiO_2	32.74	33.05	32.82	32.62	30.42	30.00	31.94
ZrO_2	61.34	61.05	61.45	61.59	59.15	58.05	60.44
HfO_2	4.24	3.42	4.23	3.14	2.476	2.135	2.94
P_2O_5	0.128	0.009	0.040	0.087	0.694	0.569	0.254
CaO	0.007	0.000	0.016	0.011	0.069	0.178	0.056
FeO	0.187	0.430	0.878	1.366	0.172	1.891	0.821
MnO	0.000	0.021	0.000	0.000	0.000	0.066	0.044
Y_2O_3	0.120	0.000	0.000	0.011	0.639	0.835	0.40
Ce_2O_3	0.027	0.089	0.000	0.028	0.000	0.000	0.048
Yb_2O_3	0.205	0.139	0.037	0.160	1.297	1.157	0.499
PbO	0.016	0.047	0.000	0.048	0.000	0.069	0.045
ThO_2	0.400	0.165	0.127	0.076	0.934	0.444	0.358
UO_2	0.187	0.000	0.057	0.117	0.149	0.172	0.155
Total	99.60	98.47	99.66	99.25	96.01	95.65	98.11
Structural formula for 4 oxygen atoms							
Al	0.000	0.001	0.000	0.000	0.000	0.002	0.001
Si	1.011	1.020	1.013	1.007	0.939	0.926	0.986
Zr	0.921	0.917	0.923	0.925	0.924	0.907	0.920
Hf	0.032	0.040	0.040	0.030	0.034	0.029	0.034
P	0.003	0.001	0.001	0.002	0.017	0.014	0.006
Ca	0.000	0.000	0.001	0.001	0.002	0.005	0.002
Fe	0.005	0.011	0.022	0.034	0.005	0.059	0.023
Mn	0.000	0.001	0.000	0.000	0.000	0.002	0.002
Y	0.003	0.000	0.000	0.001	0.013	0.017	0.011
Ce	0.001	0.002	0.000	0.001	0.000	0.000	0.001
Yb	0.004	0.003	0.001	0.003	0.027	0.024	0.010
Pb	0.001	0.001	0.000	0.001	0.000	0.001	0.001
Th	0.013	0.005	0.004	0.003	0.017	0.008	0.008
U	0.002	0.000	0.001	0.001	0.003	0.003	0.002
∑A+B	2.0	2.0	2.05	2.01	1.98	1.98	2.0
Hf / Zr	17.94	14.40	14.53	19.61	23.89	27.19	19.59
U / Th	2.14	0.00	2.23	0.65	6.27	2.58	2.77
#Hf	5.28	3.54	6.44	4.85	4.02	3.56	4.62

#Hf = 100*Hf/(Zr+Hf)

N= number of samples

known; because the phases in nature are metamict (Th and U commonly substitute for REE in minerals, as mentioned above). The smaller or Y-group (heavy) REE exhibit irregular coordination numbers with coordination number from 6 to 9, most commonly 8, whereas the larger or Ce-group (light) REE exhibit larger coordination numbers from 7 to 12, most commonly 9 (MIYAWAKI & NAKAI, 1987).

The trivalent Ce-group REE are structurally very similar to the Ca^{2+}, therefore they commonly substitute Ca in rock-forming minerals. Substitution of a trivalent REE cation for divalent Ca requires a charge compensating mechanism, i.e., a coupled substitution can be represented by the operators EuCa-1(for Eu^{2+}; add one Eu, remove one Ca or exchange Eu for a Ca), YCe_{-1}, and $CeTh_{-1}$ (for Ce^{4+}). The light rare earths (called cerium-group or LREE) have relatively large ionic radii similar to that of Ca^{2+} and Th^{4+}, in contrast to the heavy rare earths (plus Y and Mn^{2+}). All of the REE commonly substitute each other in minerals. LREE tend to be concentrated in highly fractionated basic rocks such as carbonatites (FÖRSTER,

Table 4. Mineral chemistry of selected some minerals from El-Sibai shear zone, the minerals obtained by EMPA, the major oxides by (wt%).

Rock	**El Sibai**	**El Sibai**	**El Sibai**	**El Sibai**	**El Sibai**
Sample	**Th-rich zircon Core** **MA226-E10** **Z7**	**Th-rich zircon Rim** **MA226-E10** **Z8**	**Th-rich zircon Core** **MA226-ES6** **Z9**	**Th-rich zircon Rim** **MA226-ES6** **Z10**	**Average** **N=4**
Al_2O_3	0.462	0.807	0.477	0.849	0.649
SiO_2	30.03	28.85	29.98	29.33	29.55
ZrO_2	58.07	51.60	52.91	51.20	53.47
HfO_2	3.18	2.63	4.28	2.77	3.34
P_2O_5	0.131	0.158	0.136	0.166	0.148
CaO	0.188	0.567	0.194	0.596	0.386
FeO	0.589	1.058	0.618	1.113	0.845
MnO	0.000	0.138	0.000	0.146	0.142
TiO_2	0.000	0.030	0.000	0.032	0.031
Y_2O_3	1.070	2.662	2.114	2,799	2.16
Ce_2O_3	0.099	0.228	0.102	0.240	0.167
Yb_2O_3	0.429	0.672	0.442	0.706	0.562
PbO	0.021	0.015	0.028	0.026	0.023
ThO_2	2.30	4.97	6.37	8.20	5.46
UO_2	0.362	0.710	0.374	0.746	0.548
Total	96.93	95.10	98.03	98.92	97.25
Structural formula for 4 oxygen atoms					
Al	0.010	0.017	0.015	0.027	0.017
Si	0.927	0.890	0.925	0.905	0.912
Zr	0.872	0.775	0.827	0.800	0.819
Hf	0.030	0.025	0.059	0.058	0.048
P	0.003	0.004	0.003	0.004	0.004
Ca	0.005	0.016	0.005	0.017	0.011
Fe	0.015	0.027	0.019	0.035	0.024
Mn	0.000	0.003	0.000	0.005	0.004
Ti	0.000	0.001	0.000	0.001	0.001
Y	0.022	0.056	0.044	0.058	0.045
Ce	0.002	0.005	0.002	0.005	0.004
Yb	0.009	0.014	0.009	0.015	0.012
Pb	0.001	0.001	0.001	0.001	0.001
Th	0.075	0.163	0.116	0.150	0.126
U	0.004	0.007	0.006	0.013	0.008
$\sum$A+B	2.0	2.0	2.03	2.09	2.03
Hf /Zr	18.26	19.60	12.36	18.48	17.18
U /Th	6.35	7.00	17.61	10.94	10.48
#Hf	5.98	4.85	7.48	5.13	5.86

#Hf = 100*Hf/(Zr+Hf)

N= number of samples

2000), whereas HREE and especially Y tend to be concentrated in fractionated acid rocks in example alkaline granites and pegmatites. The EMPA for these crystals reflect the cerite composition. The EPMA indicate that the mean values of major elements in cerite are Ce_2O_3 (65.48 wt%), SiO_2 (7.16 wt%), ThO_2 (9.92 wt%), CaO (2.31 wt%), Y (2.13 wt%), Yb_2O_3 (1.31 wt%), Al_2O_3 (4.55 wt%), FeO (0.23 wt%), MgO (0.2 wt%), UO_2 (0.38 wt%) and F (2.46 wt%) with significant amounts of Sr, HREE, and Hf (Fig. 5f, Table 5).

Fluorapatite $Ca_5(PO_4)_3F$

Under binocular microscope, apatite grains are mainly massive with well rounded to subrounded

Table 5. Mineral chemistry of selected some minerals from El-Sibai shear zone, the minerals obtained by EMPA, the major oxides by (wt%).

Rocks	**El-Sibai**	**El-Sibai**	**El-Sibai**	**El-Sibai**		**El-Sibai**	**El-Sibai**	**El-Sibai**	**El-Sibai**	
Sample	**MA226 ES10**	**MA226 ES10**	**MA226 ES5**	**MA226 ES6**	**Average N=4**	**MA226 ES3**	**MA226 ES3**	**MA226 ES3**	**MA226 ES3**	**Average N=4**
Mineral name	**Flourite F1**	**Flourite F2**	**Flourite F3**	**Flourite F4**		**Cerite Ce1**	**Cerite Ce2**	**Cerite Ce3**	**Cerite Ce4**	
Al_2O_3	1.118	0.461	1.103	0.455	0.786	5.45	4.23	4.70	3.82	4.55
SiO_2	0.825	0.469	0.813	0.462	0.545	9.08	6.17	7.83	5.57	7.16
Na2O	0.941	0.472	0.928	0.466	0.702	0.000	0.000	0.000	0.000	0.000
F	45.21	47.06	44.60	46.43	45.83	2.979	2.300	2.569	2.008	2.464
CaO	67.64	70.80	66.72	69.85	68.75	2.383	2.528	2.055	2.283	2.31
P_2O_5	0.061	0.081	0.060	0.080	0.068	0.133	0.156	0.115	0.141	0.136
MgO	0.000	0.011	0.015	0.010	0.012	0.215	0.223	0.124	0.255	0.2
FeO	0.010	0.012	0.000	0.012	0.012	0.258	0.225	0.222	0.203	0.227
SrO	0.000	0.012	0.000	0.010	0.011	0.009	0.015	0.012	0.018	0.014
Y_2O_3	2.661	1.207	2.625	1.190	0.920	2.711	1.813	2.339	1.637	2.125
Ce_2O_3	0.730	0.000	0.720	0.138	0.435	67.02	66.60	67.81	60.16	65.48
La_2O_3	0.059	0.140	0.058	0.000	0.086	0.120	0.074	0.104	0.067	0.091
Pr_2O_3	0.028	0.071	0.028	0.000	0.042	0.000	0.000	0.000	0.000	0.000
Nd_2O_3	0.124	0.000	0.122	0.070	0.105	0.661	0.573	0.570	0.587	0.580
Eu_2O_3	0.010	0.000	0.000	0.000	0.011	0.000	0.348	0.000	0.314	0.331
Gd_2O_3	0.100	0.000	0.099	0.000	0.099	0.000	0.000	0.000	0.000	0.10
Dy_2O_3	0.117	0.126	0.115	0.124	0.121	0.508	0.280	0.438	0.253	0.37
Er_2O_3	0.244	0.011	0.241	0.011	0.090	0.778	0.244	0.471	0.220	0.478
Yb_2O_3	0.350	0.000	0.346	0.000	0.348	1.663	1.126	1.434	1.017	1.310
HfO_2	0.000	0.120	0.000	0.119	0.120	0.000	0.021	0.000	0.019	0.07
PbO	0.000	0.049	0.000	0.048	0.048	0.000	0.000	0.000	0.000	0.000
ThO_2	0.197	0.073	0.194	0.072	0.159	7.13	13.86	6.12	12.52	9.92
UO_2	0.021	0.026	0.000	0.026	0.068	0.382	0.421	0.329	0.380	0.375
Total	101.51	101.36	99.99	100.01	100.72	99.98	100.0	96.24	90.33	96.64
Structural formula on basis of 4 oxygen atoms										
Si	0.026	0.025	0.025	0.014	0.017	0.284	0.193	0.244	0.172	0.223
Na	0.023	0.015	0.024	0.015	0.020	0.000	0.000	0.000	0.000	0.000
Al	0.029	0.010	0.023	0.010	0.018	0.114	0.088	0.098	0.080	0.095
F	------	-----	-------	-------	------	------	------	------	------	-------
Hf	0.000	0.002	0.000	0.004	0.002	0.000	0.002	0.000	0.001	0.001
P	0.002	0.002	0.002	0.002	0.002	0.003	0.004	0.003	0.004	0.004
Ca	1.88	1.97	1.853	1.940	1.91	0.070	0.070	0.057	0.063	0.033
Mg	0.001	0.001	0.001	0.001	0.001	0.007	0.007	0.004	0.008	0.006
Fe	0.000	0.004	0.000	0.001	0.002	0.008	0.007	0.006	0.006	0.007
Sr	0.000	0.001	0.000	0.001	0.001	0.001	0.001	0.001	0.001	0.001
Y	0.055	0.025	0.077	0.035	0.048	0.057	0.038	0.069	0.048	0.051
Ce	0.015	0.004	0.021	0.004	0.011	1.40	1.39	1.986	1.762	1.63
La	0.001	0.003	0.002	0.000	0.007	0.003	0.002	0.003	0.002	0.003
Pr	0.001	0.001	0.001	0.000	0.001	0.001	0.000	0.000	0.000	0.001
Dy	0.002	0.003	0.004	0.003	0.003	0.011	0.006	0.020	0.007	0.009
Nd	0.003	0.000	0.004	0.002	0.003	0.014	0.012	0.017	0.015	0.015
Eu	0.001	0.000	0.000	0.000	0.001	0.000	0.000	0.000	0.009	0.008
Gd	0.002	0.000	0.003	0.000	0.002	0.000	0.000	0.000	0.000	0.000
Er	0.005	0.001	0.007	0.004	0.004	0.016	0.005	0.020	0.007	0.012

Table 5. (continued)

Yb	0.007	0.000	0.010	0.000	0.009	0.035	0.023	0.042	0.030	0.032
Pb	0.000	0.001	0.000	0.002	0.001	0.000	0.000	0.000	0.000	0.000
Th	0.004	0.003	0.006	0.002	0.004	0.130	0.253	0.112	0.228	0.181
U	0.001	0.001	0.000	0.001	0.001	0.006	0.007	0.006	0.006	0.007
Th/U	9.38	2.81	0.000	2.81	5.00	18.66	32.92	18.66	32.90	25.86

-----not calculated

N= number of samples

shapes. The color of apatite grains generally varies from pale yellow to dark brown. The EPMA (Fig. 6a, b) reflects the chemical composition of apatite associated with minor amount of uranium (1.63 wt%) and manganese. Uranium usually substitutes for Ca in fluorapatite. According to Deer et al. (1966, 1992) the intensity of the color in fluor-apatite increases with increasing Mn content. The EMPA for these crystals reflect the zircon composition (Fig. 6b, Table 6). The EPMA indicate that the major elements in zircon are CaO (55.21 wt%), P_2O_5 (42.08 wt%), and F (2.7 wt%). Significant amounts of Th, Fe, Y and LREE were reported as substitutions in fluorapatite (Table 6).

Other minerals

Monazite [LREE,Th(PO_4)] is the most common accessory mineral in many magmatic and metamorphic rocks, especially rocks characterized by mildly to strongly peraluminous compositions. Monazite crystals appear mainly as euhedral to subhedral inclusions in the zircon and columbite minerals (Fig. 6a).

Pyrite (FeS_2) is the main sulfide encountered and it is disseminated in the shear zones. Generally, pyrite of the El-Sibai shear zones is partially or entirely oxidized to oxyhydroxides such as hematite and goethite. This process can be classified as pseudomorphic desulfidization under oxidizing conditions. Desulfidization of pyrite precursor creates voids that can be refilled by secondary minerals enriched in Th, REE, U and Ti. Pyrite occurs as well developed cubic octahedron crystals with pale-brass yellow colour and metallic luster. This confirms the reducing conditions during the late stages of columbite crystallization, which is also responsible for the formation of pyrite. This may explain the metasomatic processes that took place under alkaline medium.

Titanite CaTi(SiO_4)(O,OH,F) is an important constituent of ijolitic and nepheline syenitic alkaline rocks. Amounts of trace elements, particularly the LREE, Nb, Ta and Zr, titanite and other accessory phases such as apatite and perovskite are important in the study of the genesis and geochemical evolution of alkaline igneous rocks. Titanite is an important factor controlling the REE distribution in a wide variety of rock compositions and geochemical processes because it is one of the most common and pervasive accessory phases and it has the ability to incorporate large quantities

Table 6. Mineral chemistry of selected some minerals from El-Sibai shear zone, the minerals obtained by EMPA, the major oxides by (wt%).

Rocks	**El-Sibai**	**El-Sibai**	**El-Sibai**	**El-Sibai**	**El-Sibai**
Sample	**ZS6-1**	**ZS6-1**	**ZS6-1**	**ZS6-1**	
Mineral name	**Fluorapatite Core-A1**	**Fluorapatite Rim-A2**	**Fluorapatite Core-A3**	**Fluorapatite Rim-A4**	**Average N=4**
F	2.154	2.156	2.744	2.242	2.324
SiO_2	0.086	0.140	0.211	0.327	0.191
MgO	0.016	0.019	0.014	0.020	0.018
CaO	54.75	55.19	54.40	56.48	55.21
P_2O_5	41.51	42.16	41.43	43.20	42.08
Cl	0.147	0.144	0.222	0.285	0.2
FeO	0.088	0.297	0.278	2.36	0.756
SrO	0.000	0.014	0.033	0.047	0.031
Y_2O_3	0.000	0.009	0.000	0.011	0.011
La_2O_3	0.096	0.032	0.020	0.043	0.048
Ce_2O_3	0.043	0.000	0.062	0.097	0.067
Pr_2O_3	0.110	0.000	0.022	0.044	0.059
Nd_2O_3	0.080	0.000	0.150	0.341	0.19
Sm_2O_3	0.029	0.000	0.000	0.000	0.029

Table 6. (continued)

Gd_2O_3	0.113	0.000	0.000	0.000	0.113
PbO	0.091	0.056	0.000	0.000	0.088
ThO_2	0.020	0.000	0.041	0.081	0.047
UO_2	0.000	0.000	0.000	0.000	0.000
Total	98.38	99.27	98.40	104.0	100.01
Structural formula on basis of 4 oxygen atoms					
F	------	-------	-------	--------	------
Mg	0.001	0.001	0.001	0.001	0.001
Si	0.003	0.004	0.006	0.010	0.006
P	1.038	1.054	1.036	1.080	1.05
Cl	-------	-------	-------	-------	------
Ca	0.978	0.986	0.971	1.008	0.986
Fe	0.003	0.009	0.009	0.074	0.024
Sr	0.000	0.001	0.001	0.002	0.001
Y	0.000	0.001	0.000	0.001	0.001
La	0.001	0.000	0.002	0.003	0.001
Ce	0.003	0.001	0.001	0.001	0.002
Pr	0.003	0.000	0.001	0.001	0.002
Nd	0.002	0.000	0.000	0.000	0.005
Sm	0.001	0.000	0.000	0.000	0.001
Gd	0.003	0.000	0.000	0.000	0.003
Pb	0.002	0.001	0.000	0.000	0.002
Th	0.001	0.000	0.001	0.000	0.001
U	0.000	0.000	0.000	0.000	0.000

-----no calculation

N= number of samples

of LREE in its crystal structure (Henderson, 1980; Seifert & Kramer, 2003).

Hematite (Fe_2O_3) appears most commonly in igneous rocks, especially in the mineralized granites. It is also very important in sedimentary rocks and their more metamorphosed equivalents (Deer et al., 1966). In the mineralized shear zone of El-Sibai peralkaline granites, hematite occurs as a secondary phase of magnetite crystals in the form of aggregates with thorite and zircon minerals.

Disscussion

Accessory minerals that have crystallized from magma display different stabilities during fluid-induced, pervasive late-magmatic to hydrothermal alteration that normally affect granites. Intergrowths of thorite and zircon are abundant in the alkali-feldspar granites (Figs. 3a, 7). Zircon and thorite crystallize in space group I41/amd (Taylor & Ewing, 1978; Hazen & Finger, 1979). Their structures consist of chains of alternating edge-sharing SiO_4 tetrahedra and MeO_8 (Me=Zr or Th) triangular dodecahedra extending parallel to [001] and linked by edge-sharing MeO_8 polyhedra. The structural modifications also affect the behavior of zircon and thorite during high- and low-T alterations. Solid-solution ranges between thorite and zircon were identified in the present study (Fig. 8). These ranges (from Th-rich zircon to zircon) could be connected to the high-T fluid-induced alteration of precursor minerals. Some thorite and zircon crystals have compositions close to ideal stoichiometry, on the contrary others show varying degrees of alteration. Based on 4 oxygen atoms, the calculated formula of zircon is $^{A}(Zr_{0.92}\ Hf_{0.034}Th_{0.008}U_{0.002}Ca_{0.002}Fe_{0.023}Pb_{0.001})\ ^{T}_{\Sigma\ 0.99}\ ^{B}(Si_{0.99}P_{0.006}\ Al_{0.056})_{\Sigma\ 1.01}O_4$, where Th, Si and Zr represent the principle elements with considerable amounts of Ca, U, Fe, and trace Pb. The calculated formula of Th-rich zircon is $^{A}(Zr_{0.82}Hf_{0.05}Th_{0.126}U_{0.008}Ca_{0.011}Fe_{0.024})\ ^{T}_{\Sigma 0.91}\ ^{B}(Si_{0.91}P_{0.004}\ Al_{0.017})_{\Sigma 0.93}O_4$.

Zircon and Th-rich zircon have higher sum of all cations per formula (2.06 and 2.05 apfu, respectively) than that of ideal thorite and zircon (2 apfu, for 4 oxygen atoms). This is in agreement with Hoskin et al. (2000), Finch & Hanchar (2003) and Förster (2006), who noted that the sum of all cations per formula unit in thorite and zirconmay be N2, when these phases contain substantial amount of interstitial cations such as Ca, U and Al. Enrichment in the latter elements, in addition to F, is believed to have been introduced into the zircon–thorite system during solid state alteration, rather than during primary igneous crystallization. Solubility andmobility of Zr and Th fromthese phases require a pH between 5 and 6, at which they form $Zr(OH)_4$ complexes. At more basic pH the obtained complex changes to $Zr(OH)_5$ and the solubility increases strongly. The elevated alkalinity in the hydrothermal solutions plays an important role. The hydrothermal solution could be of magmatic origin representing residual fluids expelled from F-rich melts. This conclusion is supported by the widespread fluorite mineralization associated with Fe-oxides and dendritic Mn-oxides along joint planes. Uranium bonding within the crystal structure of thorite and zircon is not expected to be easily dissolved by the mobilizing low-T solutions (Murakami et al., 1991). It is thus likely that these minerals underwent some changes by a metamictization process. During this process U could be released from the crystal lattices. Metamictization was largely caused by nucleic recoil of U and Th during alpha decay. The bombardment of the crystal lattice by large nuclei progressively distorts and eventually destroys the crystal lattice (Murakami et al., 1991).

Zircon enriched in Hf in peralkaline granite was connected to post-magmatic metasomatic activity rather than to magmatic fractionation (Wang et al., 2000). This may be confirmed by the fact that normal fractionation during evolution of the peralkaline melt does not result in separation of Zr and Hf and hence the Zr/Hf ratio is retained at a constantly high value (e.g. approx. 20 in El-Sibai peralkaline granite). Thus, Hf-enrichment in the El-Sibai altered granite association and hence in the associated hafnian zircon is controlled by other factors. Very important is F in the evolution of such highly fractionated melts that tend to be enriched in Na and Al with decreasing silica. Fractionation includes a combination of crystal settling and flow accumulation of progressively evolved, more F-rich, lower-temperature, less dense, less viscous melts towards the upper and inner parts of the magma chamber. This leads to an increase in diffusion rates of HFSE, thus permitting late liquid–liquid fractionation of granitic melt (Hannah & Stein, 1990). The #Hf ratios (Table 3), ranging between 3.54 and 6.44 with average 4.62 in the investigated zircon of metasomatized peralkaline granites, is not so high, which manifests that an alkaline and relatively high temperature >425 °C (Abdalla et al. 1994) environment could be suitable for their deposition, in which the Hf-complexes are thermally unstable (Portnov, 1965).

Zircon of the El-Sibai altered peralkaline granites is closely concordant with the trends III and MHZ (Figs. 8, 9) that presumably represent a preserved metasomatic hydrothermal trend. This trend deviates from the theoretical trend exhibited by the zircon-hafnon solid solution series (i.e. trend I, Fig. 8). This discrepancy can be attributed to a significant deficit of Zr and Hf relative to Si content (i.e. high concentration of vacancies on the Zr lattice position (Kempe et al., 1997; Abdalla et al., 2008).

The trends III and MHZ (Figs. 8, 9) exhibited by zircons from metasomatized hydrothermal environment are in accordance with the trend defined by the substitution scheme Zr^{4+}, $(Si^{4+}) \leftrightarrow Hf^{4+} + HREE^{3+} + U^{4+} + Th^{4+} + Y^{3+} + (P^{5+})$. According to Speer (1982) and Belousova et al. (1998) zircon is unusual composition occurring along such a trend. These zircons were interpreted by Pointer et al. (1988) as metastable solid solution, in the series zircon-xenotime (YPO_4), thorite ($ThSiO_4$), coffinite ($USiO_4$). Minerals of this series are isostructural and can show limited substitution range with zircon even at higher temperature (Mumpton & Roy, 1961). Because the HREE are geochemically close to Y, they also tend to be involved in this isomorphic substitution series. This zircon is formed from fluids that transported Th, U, Y, P, and HREE. Zircon is highly soluble in alkalic and F-rich magmas (Keppler, 1991), therefore Zr is progressively enriched in differentiating magmas. Over a range of 0-6 wt% F, solubility of zircon increases with the square of the F content, and the solubility of other refractory minerals, including rutile and thorite also increases (Keppler, 1991). Zircon crystallization removes most Zr from the magma. Zircon is extremely stable, even during most hydrothermal alterations, which inhibit subsequent mobilization. In contrast, sodic pyroxenes and amphiboles are more easily broken down and there Zr would be easily released to hydrothermal fluids (Rubin et al., 1993). Susceptibility of zircon to alteration can be enhanced by metamictization or mechanical fracturing during deformation.

Ferrugination (hematitization) process is mainly related to strongly alkaline hydrothermal solutions at pH value of more than 10 with temperatures varying between 350 °C and 450 °C (Sweewald & Sayfried, 1990), while kaolinitization and silicification processes are essentially associated with strongly acidic solutions at pH from 1 to 3 with temperatures varying between 150 °C and 400 °C (Bucanan, 1982). Accordingly, the temperatures of the solution ranged between 150 °C and 450 °C. It is believed that the mineralizing hydrothermal solutions never reached more than 500 °C due to destruction of Al_2O_3 above this temperature (Frantz & Weisbrod, 1974). Ferrugination along the shear zone was accompanied by higher intensity of radioactivity compared to the silicification and kaolinitization processes (Fig. 3). This is due to the high ability of iron oxides to adsorb radioactive elements from its solutions. The reported ferrugination process may be due to the mobilization of ferric ions released from the ferromagnesian minerals during the alteration processes. Hematite may be precipitated according to the oxidation- reduction reaction.

$$4\ Fe_3O_4\ \textit{(Magnetite)} + O_2 \rightarrow 6\ Fe_2O_3\ \textit{(Hematite)}$$

Silicification process in a shear zone is also well developed and most commonly represented by quartz veinlets varying in thickness from a few mm to less than 20 cm, extending for variable distances, not exceeding 80 m. The silicification process results in an increase of SiO_2 at the expense of the other major oxides. Pier (1992) attributed the development of SiO_2 to the hydration of feldspars as follows:

$$75Na_2CaAl_4Si_8O_{24} + 2H^+ + K^+\ \textit{(Plagioclase)} \rightarrow KAl_3Si_3O_{10}(OH)_2 + 1.5Na^+ + 0.75Ca^{+2} + 3SiO_2\ \textit{(Muscovite)}$$

$1.5KAlSi_3O_8 + H^+$ *(Potassium feldspar)* $\rightarrow 0.5\ KAl_3Si_3O_{10}(OH)_2 + K^+ + 3SiO_2$ *(Muscovite)*

Kaolinitization accompanies, but to a less extent, the ferrugination and silicification alterations in the shear zone. The kaolinitization process causes an increase in the amount of Fe_2O_3, CaO and MnO at the expense of the other major oxides. The intensity of kaolinite alteration increases near the edge of the shear zone. Rice (1973) pointed out that kaolinite may be formed in granite due to hydrolysis of albite. In this reaction silica precipitates as an amorphous phase.

$4NaAlSi_3O_6 + 4H_2CO_3 + 18H_2O$ *(Albite)* $\leftrightarrow 4Na^+ + 8H_4SiO_4 + 4HCO_3 + Al_4Si_4O_{10}(OH)_8$ *(Kaolinite)*

Crystallization of fluorite, galena and pyrite in the mineralized shear zone reflects the important role of F and S. Zr, Hf, Th and Ti are typical HFSE, which are generally considered immobile during hydrothermal water-rock interactions. Experimental and natural evidences, however, have demonstrated that Zr, Ti and Th may become mobile especially in high-temperature (magmatic or hydrothermal) environments containing strong complexing agents such as fluorine, sulfur and others (Keppler, 1993). The mobility of the REE and Th was attributed to high F contents in the hydrothermal fluids (Poitrasson, 2002) as F-rich fluids are capable of transporting Th (Keppler & Wyllie, 1990). The critical role of F complexing in REE transport in hydrothermal fluids is also indicated by Y, Ho fractionation (Bau & Dulski, 1995). The fact that F may play a prominent role in the hydrothermal mobilization of HFSE has been indicated for Zr, Th and REE (Moine & Selvi, 1999). Harris & Marin (1980) reported on the important role of mobile fluoride complexes such as $[Na(REE)F_4]$ and $[(ZrF)(REEF_4)_3]$ in determining the distribution of REE and other trace elements such as Zr during hydrothermal conditions. Moreover, Taylor et al. (1981) added carbonate complexes in the alkali-enriched fluid as an important factor responsible for Zr and HREE transportation. The abundantly detected zircon and Th-bearing minerals, of demonstrably hydrothermal origin, can be attributed to the role of F-rich fluids. Zr and Th are generally considered as highly immobile elements, yet the occurrence of zircon indicates that their significant concentrations can be transported via specified F-rich fluids.

Pichavant (1983) showed that the F-rich fluid phase equilibrated with alkali feldspars, is strongly enriched in Na in comparison to the Cl-rich fluid. Thus any process leading to reduction of F-rich fluid (such as volatile loss or stabilizing F into F-bearing minerals, e.g. fluorite, and fluorapatite), will result in the albitization of the granite. Consequently, an increased pH of the exsolved fluids from the crystallizing peralkaline granite will lead to the destabilization of rare element complexes including those of Zr and Hf in these fluids and promote their deposition. Zircon and xenotime are isostructural and exhibits the general formula ABO_4, where A refers to the larger Zr and Y atoms and B to the smaller P and Si atoms. Xenotime-substituted zircon is formed as the result of the coupled substitution:

$Zr^{4+} + Si^{4+} \rightarrow Y(HREE)^{3+} + P^{5+}$ (Romans et al., 1975).

Conclusion

Mineralized shear zone trending NNE-SSW is located at the northern segment of Gabal El-Sibai peralkaline granites (500 m in length and 0.5 to 1.5 m in width). Ferrugination, kaolinitization, and silicification are the main wall-rock alteration features developed within the shear zone. There the rare-metal minerals are associated with ferrugination (hematitization) zone. These alterations are good traps for rare metals of thorite, ferrocolumbite, pyroclore, plumbopyroclore, fluorite, cerite-(Ce), zircon, Th-rich zircon, zirconolite (mixture of zircon and columbite), fluorapatite, titanite, and monazite minerals. Cerite-(Ce), zirconolite and plumbopyroclore minerals are represented the first time in the rare-metals peralkaline granites in the Eastern Desert of Egypt.

Electron probe microanalysis (EPMA) provides an indication of a range of solid solutions between thorite and zircon, in which intermediate phases, i.e. Th-rich zircon, were formed. These phases have higher sum of all cations per formula (2.0 to 2.09 apfu, for 4 oxygen atoms) than that of ideal thorite and zircon. This is attributed to the presence of substantial amount of interstitial cations such as U, Y, Ca, and Al in these phases. Enrichment of Th and U in an altered zircon (Th-rich zircon) preferentially involves coupled substitution $Ca^{2+} + (Th,U)^{4+} \leftrightarrow 2Zr^{4+} + 2Si^{4+}$, implying that significant amount of U and Th may enter the Zr and Si position in zircon. Although Zr, Hf, and HREE are considered as highly immobile elements, yet the occurrence of the formed Zircon enriched Hf-, U-, Th-, Y- and HREE of hydrothermal origin indicates the mobilization of these elements via specified (K^+, Na^+, H^+, CO^{3-}, O_2 and F^-)-rich fluids.

This study shows zircon and Th-rich zircon related to metasomatic hydrothermal zircon (MHZ). Zircon and fluorite of demonstrably hydrothermal origin can be attributed to the role of fluorine-rich fluids. Fluoride complexes such as $[Na(REE)F_4]$ and $[(ZrF)(REEF_4)_3]$ are important to determine the distribution of REE and other trace elements, such as Zr during hydrothermal conditions. Zr and Th are generally considered as highly immobile elements, yet the occurrence of zircon indicates that significant concentrations of Zr and Th can be transported under specified F-rich fluids. The zircon of El-Sibai altered peralkaline granite is interpreted as a metastable solid solution, in the series zircon–thorite ($ThSiO_4$). The Hf-concentrating mechanism is assumed due to solid-state action (subsolidus reaction) of exsolved fluids rich in K^+, Na^+, F^- and subsequently H^+.

The shear zone was affected by different types of hydrothermal solutions with temperatures varying between 150 °C and 450 °C. The produced alterations acted as good traps for Th- and U-bearing minerals with rare metals in the El-Sibai peralkaline granites (shear zone). The detailed mineralogical investigations of these zone revealed its enrichment in Th, Zr, Nb, Pb, U, F, P, LREE (Ce), especially concerning the hematization processes. The close correlation of ferruginated samples with high radioactivity is related to the high ability of iron oxides to adsorb radioactive elements from their solutions.

The shear zone facilitates the circulation of hydrothermal fluids, leading to mobilization and redistribution of radioactive elements. Also the presence of galena and deep violet fluorite are very good evidences for the presence of hydrothermal fluids. Therefore, it is clear that alteration processes have resulted from ascending (hypogene) hydrothermal solutions rather than descending (supergene) meteoric water. So, the hydrothermal origin could be accepted for mineralizations within the shear zone.

From the study of El-Sibai altered granites (shear zone), we concluded that the studied area contains high concentrations of Th, Zr, Nb, U, Pb, P, Ce, F and REE, especially in the ferruginated parts of the area. Accordingly, the El-Sibai shear zone could represent a favorable source for rare metals (Th, Zr, Nb, U, Pb, P, Ce, F, and REE).

References

Abadalla, H. M., Helba, H. & Matsueda, H. 2008: Chemistry of zircon in rare metal granitoids and associated rocks, Eastern Desert, Egypt, Resource Geology, 59/1: 51-68, doi:10.1111/j.1751-3928.2008.00079.x.

Abdalla, H.M., Matsueda, H., Ishihara, S. & Miura, H. 1994: Mineral chemistry of albite-enriched granitoids at Um Ara, Southeastern Desert, Egypt. Int. Geol. Re., 36/11: 1067-1077, doi:10.1080/00206819409465505.

Abdel-Fattah, M., Abdel-Rahman, A.M. & El-Kibbi, M.M. 2001: Anorogenic magmatism: chemical evolution of the Mount El-Sibai A-Type complex (Egypt), and implications for the origin of within-plate felsic magmas, Geological Magazine, 138: 67-85.

Abdel Kader, Z.M., Bakhit, F.S. & Ali, M.A. 2001: Geochemistry of the younger granites in El Sibai area, Central Eastern Desert, Egypt, The Mineralogical Society of Egypt. The Fourteenth Annual Meeting, Abstract: 16 p

Abd El-Naby, H. H. 2009: High and low temperature alteration of uranium and thorium minerals, Um Ara granites, South Eastern Desert, Egypt, Ore Geology Reviews, 35: 436-446.

Ali, M.A. 2001: Geology, petrology and radioactivity of Gabal El-Sibai area, Central Eastern Desert, Egypt, Ph. D. Thesis, Cairo University: 300 p.

Ali, M.A. & Lentz, D. R. 2001: Mineralogy, geochemistry and age dating of shear zones hosted Nb-,Ta-, Zr-Hf-, Th-, U-bearing granitic rocks at Ghadir and El-Sella areas, South Eastern Desert, Egypt, Chin. J. Geochem., 30/4: 453–478, doi:10.1007/s11631-011-0531-5.

Bayliss, P., Mazzi, F., Munno, R. & White, T. J. 1989: Mineral nomenclature: Zirconolite. Mineral Mag., 53: 565-569.

Bayliss, P. & Levinson, A. A. 1988: A system of nomenclature for rare-earth mineral species: Revision and extension. Am. Mineral., 73: 422-423.

Bau, M. & Dulski, P. 1995: Comparative study of yttrium and rareearth element behaviours in fluorine-rich hydrothermal fluids. Contrib. Mineral. Petrol., 119: 213–223.

Belousova, E. A., Griffin, W. L. & Pearson, N. J. 1998: Trace element composition and cathodoluminescence properties of Southern African kimberlitic zircon. Mineral Mag., 62: 355–366.

Brugger, J., Gieere, R., Graeser, S. & Meisser, N. 1997: The crystal chemistry of roméite. Contrib. Mineral. Petrol., 127: 136-146.

Butler, C. A., Holdsworth, R. E & Stachan, R. A. 1995: Evidence for Caledonian sinistral strike-slip motion and associated fault zone weakening, Outer Hebrides fault zone, NW Scotland. Journal of Geological Society, London, 152: 743-746.

Bucanan, M. S. 1982: The geochemistry of some igneous rock series. Geochimica et Cosmochimica Acta, 9: 101-137.

Breiter, K., Förster, H. J. & Škoda, R. 2006: Extreme P-, Bi-, Nb-, Sc-, U- and F-rich zircon from fractionated perphosphorous granites: the peraluminous Podlesí granite system, Czech Republic. Lithos, 88: 15–34.

Chakoumakos, B. C. 1984: Systematics of the pyrochlore structure type, ideal. J., Sol. State, Chem, 53: 120-129.

Chakoumakos, B. C. 1986: Pyrochlore. In McGraw-Hill Yearbook of Science and Technology 1987. Parker, S. P. (ed.): McGraw-Hill, New York: 393-395.

Correia Neves, J.M., Nunes, J.E. & Sahama, T.G. 1974: High hafnium members of the zircon-hafnon series from the granite pegmatites of Zambezia, Mozambique, Contrib. Mineral. Petrol., 67: 73-80.

Černˊy, P., Meintzer, R. E. & Anderson, A. J. 1985: Extreme fractionation in rare-element granitic pegmatites: Selected examples of data and mechanisms. Candian Mineralogist, 23: 381–421.

Deer, W. A., Howie, R. A. & Zussman, J. 1966: An introduction to rock forming minerals. Longmans, London: 517 p.

Deer, W. A., Howie, R. A. & Zussman, J. 1992: Rock forming minerals, 5. Non silicates, John Wiley & Sons, New York: 371 p.

El-Gaby, S. 1975: Petrochemistry and geochemistry of some granites from Egypt. Neu. Jb. Miner. Abh., 124: 147-189.

El-Ramly, M. F. 1962: The absolute ages of some basement rocks in the Eastern and Southwestern Deserts of Egypt. Geological Survey of Egypt paper, 15: 12 p.

El-Ramly, M.F. & Akaad, M.K. 1960: The basement complex in the Central Eastern Desert of

Egypt between lat. 24° 30’ and 25° 40’ N. Geological. Survey, Egypt. P., 8: 35 p.

El-Shazly, E. M. 1964: On the classification of the Precambrian and other rocks of magmatic affiliation in Egypt. XXII Inter. XXII Inter. Geol. Congr. Proc. Sect. 10, India, 88-101.

El-Kammar, A. M., EL-Hazik, N. S., Mahdi, M. & Ali, N. 1997: Geochemistry of accessory minerals associated with radioactive mineralization in the Central Eastern Desert, Egypt. Journal of African Earth Sciences, 25/2: 237-252.

El-Manharawy, M. S. 1977: Geochronological investigation of some basement rocks in Central Eastern Desert, Egypt between lats. 25° 00 and 26° 00 N. Ph. D. Thesis, Fac. Sci., Cairo University: 238 p.

Finch, R. J. & Hanchar, J. M. 2003: Structure and chemistry of zircon and zircon group minerals. In: Hanchar, J.M. & Hoskin, P.W.O. (eds.): Zircon. Reviews in Mineralogy and Geochemistry, Mineralogical Society of America, Geochemical Society, Washington, DC 53: 26 p.

Förster, H. J. 2006: Composition and origin of intermediate solid solutions in the system thorite–xenotime–zircon–coffinite. Lithos, 88: 35–55.

Förster, H. J. 2000: Cerite-(Ce) and thorian synchysite-(Ce) from Niederbobritzsch (Erzgebirge, Germany): implications for the differential mobility of Th and the LREE during granite alteration. Canadian Mineralogist, 38: 67–79.

Fleischer, M. 1987: Glossary of Mineral Species, 5th Edition. Mineral. Rec, Inc., 227, Tucson, AZ.

Fleischer, M. 1989: Additions and corrections to the Glossary of Mineral Species, 5th Edition. Mineral. Rec., 20 (1987): 289-298.

Frantz, J. D. & Weisbord, A. 1974: Infiltration metasomatism in the system K_2O-SiO_2-Al_2O_3-H_2O-HCl. In: Geochemical transport and kinetics, 634: 261-271.

Frondel, J. W. & Cuttito, A. 1955: Glossary of uranium and thorium-bearing minerals. Geological Survey Bulletin, 5: 1009.

Gaines, R. V., Skinner, H. C. W., Foord, E. E., Mason, B., Rosenzweig, A., King, V.T. & Dowty, E.1997: Dana’s New Mineralogy. 8th ed. Wiley and Sons, New York: 1819 p.

Greiling, R.O., El-Ramly, M.F., Rashwan, A.A. & Kamal El-Din, G.M. 1993: Towards a comprehensive structural synthesis of the (Proterozoic) Arabian Nubian Shield in E. Egypt. In: U-Thorweihe & H. Schandelmeie (eds.); Geoscientist Res. Northeast Africa. Balkema, Rotterdam, 15-19.

Hannah, J.L. & Stein H.J. 1990: Magmatic and hydrothermal processes in ore-bearing systems. In: Stein, H. & Hannah, J. (eds.): Ore-bearing granite systems: Petrogenesis and mineralizing processes. Geol. Soc. Am. Spec. Paper, 1-11.

Hassan, M. A. & Hashad, A. H. 1990: Precambrian of Egypt. “The anorogenic alkalic rocks, South Eastern Desert, Egypt”. Annal Geological Survey of Egypt, 9: 81-101.

Hazen, R. M. & Finger, L.W.1979: Crystal structure and compressibility of zircon at high pressure. Am. Mineral., 64: 157–161.

Hoskin, P. W. P. O., Kinny, P. D., Wyborn, D. & Chappell, B.W. 2000: Identifying accessory mineral saturation during differentiation in granitoid magmas: an integrated approach. Journal of Petrology, 41: 1365–1396.

Henderson, P.1980: Rare earth element partitioning between sphene, apatite and other coexisting minerals of the Kangerdlugssuaq intrusion, E. Greenland. Contrib. Mineral. Petrol., 72: 81–85.

Hussein, H. A. 1978: Lecture course in nuclear geology: 101 p.

Hussein, A. A., Ali, M. M. & El-Ramly, M. F. 1982: A proposed new classification of the granites of Egypt. Journal Volcanic Geoth., Re., 14: 187-198.

Hume, W.F.1935: Geology of Egypt. Vol II, Part II. The later plutonic and intrusive rocks, Geological Survery Egypt, Government press, Cairo, 301-688

Ibrahim, I.H., Ali, M.A. & Abdel Wahed, A.A. 2003: Mineralogical and spectrometric studies of El-Sibai shear zone, Central Eastern Desert, Egypt. 6th Intern. Conf. on Geochemistry. Alex. Univ., Egypt, I-A: 25-43.

Kamal El-Din, G.M.1991: Geochemistry and tectonic significance of the Pan-African El-Sibai window, Central Eastern Desert, Egypt. Ph.D. Thesis, Heidelberg University:114 p.

Keppler, H. 1991: Influence on the solubility of high field strength trace elements in granitic melts. Eos Trans. Am. Geophys. Union, abstract 72: 532-533.

Keppler, H. 1993: Influence of fluorite on the enrichment of high field strength trace elements in granitic rocks. Contrib. Mineral. Petrol., 114: 479-788.

Keppler, H. &.Wyllie, P. J. 1990: Role of fluids in transport and fractionation of uranium and thorium in magmatic processes. Nature 348:531-533, doi:10.1038/348531a0.

Kempe, U., Gruner, T., Renno, A.D. & Wolf, D. 1997: Hf- rich zircons in rare-metal bearing granites: Magmatic or metasomatic origin. In: Papunen, H. (ed.): Mineral deposits: Research and exploration where do they meet? A.A. Balkema, Rotterdam, 643-646.

Lumpkin, G.R., Hart, K.P., McMlinn, P.J., Payne, TE., Gieré, R. & Williams, C.T. 1994: Retention of actinides in natural pyrochlores and zirconolite. Radiochim. Acta, 66/67: 469-474.

Lumpkin, G.R. & Ewing, R.C. 1995: Geochemical alteration of pyrochlore group minerals: Pyrochlore subgroup. Am. Mineral., 80: 732-743.

Mandarino, J.1999: Fleischer’s Glossary of Mineral Species. Mineralogical Recored, Tucson, Arizona.

Miyawaki, R. & Nakai, I. 1987: Crystal structures of rare-earth minerals. Rare Earths (Kidorui), 11:1-133.

Moghazi, A.M., Hassanen, M.A., Mohamed, F.H. & Ali, S. 2004: Late Neoproterozoic strongly peraluminous leucogranites, South Eastern Desert, Egypt-petrogenesis and geodynamic significance. Mineralogy and petrology, 81: 19-41.

Moine, B. & Salvi, S. 1999: Role of fluorine-rich fluids in the hydrothermal transport of “immobile” elements (Th, Zr, REE, Zl). Bull. De liaison de la Societe Francaise de Mineralogie et de Cristallographie (S. F. M. C.), 11: 90-92.

Moussa, E.M. 2001: Petrographical and geochemical characteristics of Gabal El-Sibai and Abu Garadi alkali feldspar granite phase and their potentialities to host uranium-thorium mineralization. Egyptian Mineralogist, 13: 101-124.

Moussa, E. M., Stern, R. J., Manton, W. I & Ali, K. A. 2008: SHRIMP zircon dating and Sm/Nd isotopic investigations of Neoproterozoic granitoids, Eastern Desert, Egypt. Precambrian Research, 160: 341–356.

Murakami, T., Chakoumakos, B. C., Ewing, R. C., Lumpkin, G. R. & Weber, W. J. 1991: Alphadecay event damage in zircon. Am. Mineral., 76: 1510–1532.

Pier, C.A 1992: Geochemistry of granites and trachytes from the Summit region of Mt. Kenya. Contrib. Mineral. Petrol., 89: 394-409.

Pichavant, M. 1983: (Na, K) exchange between alkali feldspars and aqueous solutions containing borate and fluoride anions, experimental results at p=1 kbar. 3rd. NATO Adv. Stud. Inst. Feldspars and feldspathoids, Rennes. XXX: 102 p.

Pointer, C.M., Ashworth, J.R. & Ixer, R.A. 1988: The zircon thorite mineral group in metasomatized granite, Ririwai, Nigeria. 1: Geochemistry and metastable solid solution of thorite and coffinite. Mineral. Petrol., 38: 245-262.

Poitrasson, F.2002: In situ investigations of allanite hydrothermal alteration: examples from calc-alkaline and anorogenic granite of Corsica (southeast France).Contri. Mineral. Petrol., 142: 485-500.

Portnov, A.M. 1965: The zirconium: hafnium ratio in minerals of the Burpala massif. Geochem Int., 2: 238–241.

Rice, C.M.1973: Chemical weathering on the Carnmenellis granite. Mineralogical Magazine, 39: 429-447.

Romans, P. A., Brown, L. & White, J. C. 1975: An electron microprobe study of yttrium, rare earth and phosphorous dis tribution in zoned and ordinary zircon. Am. Mineral., 60: 475-480.

Rubin, J. N., Henry, C. D. & Price, J. G. 1993: The mobility of zirconium and other “immobile” elements during hydrothermal alteration. Chemical Geology, 110: 29-47.

Seifert, W. & Kramer, W. 2003: Accessory titanite: an important carrier of Zr in lamprophyres. Lithos, 7: 81–98.

Smith, D. K. J. 1984: Uranium mineralogy. In: DeVivo, B., Ippolito, F., Capaldi, G. & Simpson, P.R. (eds.): Uranium geochemistry, Mineralogy, Geology, Exploration and Resources, Institute of Mining and Metalluragy, London, 43-88.

Speer, J. A. 1982: The actinide orthosilicates. In: Ribbe, P. H. (ed.): Reviews in Mineralogy, Mineralogical Society of America, 5, 2nd Edition, 113-135.

Stern, R. J. & Hedge C. E.1985: Gechronologic and isotopic contraints on Late Precambrain crustal evolution in the Eastern Desert in Egypt. Am. Journal Science, 258: 97-127.

Sultan, M., Arvidson, R.E., Duncan, I. J., Stern, R.J. & El-Kalioubi, B. 1988: Extension of the Najd shear system from Saudi Arabia to the central Eastern Desert of Egypt based on integrated field and landsat observations. Tectonics, 7/6: 1291-1306.

Sweewald, J. S. & Sayfried, J. W. 1990: The effect of temperature on metal mobility in subsea floor hydrothermal systems: constraints from basalt alteration experiments. Earth Planet Science, 101: 388-403.

Taylor, M. & Ewing, R. C. 1978: The crystal structure of $ThSiO_4$ polymorphs: huttonite and thorite. Acta Crystallographica B 34, 1074–1079.

Taylor, R. P., Strong, D. F. & Fryer B. J. 1981: Volatile control of contrasting trace element distributions in peralkaline granitic and volcanic rocks. Contrib. Mineral., Petrol., 77: 267–271.

Wang, R. C., Zhao, G. T., Lu, J. J., Chen, X. M., Xu, S. J. & Wang, D. Z. 2000: Chemistry of Hf-rich zircons from the Laoshan I- and A-type granites, Eastern China. Mineralogical Magazine, 64: 867 – 877.

Warner, J. K. & Ewing, E. R.1993: Crystal chemistry of samarskite. Am. Mineral., 78: 419-424.

Wedepohl, K. H. 1978: Handbook of geochemistry. Springer Verlag, Berlin: 478 p.

Whittaker, E. J. & Muntus, R. 1970: Ionic radii for use in geochemistry. Geochimica et Cosmochimica Acta, 34: 945.

Williams, J. k. & Gieré, R.1996: Zirconolite a review of localities worldwide, and a compilation of its chemical compositions. Bull. Nat. Hist. Museum Geol. Ser., 52: 1-24

Woodhead, J. A., Rossman, G. R. & Thomas, A. P. 1991: Hydrous species in zircon. Am. Mineral., 76: 1533-1546.